THE PREDICTION OF EXTRATROPICAL WEATHER SYSTEMS - SOME SENSITIVITY STUDIES

A.J. Simmons and M.J. Miller
European Centre for Medium-range Weather Forecasts
Reading, United Kingdom

Summary

Examples are given of the prediction of a range of extratropical weather systems using the global ECMWF spectral model. Most cases have been the subject of sensitivity experiments, and the impacts of changes in one or more aspects of the forecasting system such as model resolution, the parametrizations of convection and vertical diffusion, the orographic representation and data analysis are discussed. The cases chosen and sensitivities presented serve to illustrate the importance of particular dynamical and physical mechanisms which are discussed in the theoretically- and observationally-based papers in these proceedings.

1. INTRODUCTION

In preceding contributions to these Proceedings, accounts have been given of the nature of extratropical cyclogenesis and blocking from theoretical and observational viewpoints, including results from detailed diagnosis of specific numerical experiments. Here we consider the numerical prediction of such extratropical weather systems, with particular emphasis on cyclone development. We do not seek to present a comprehensive account of predictability in the extratropics, but rather discuss a range of cases which have been the subject of recent attention and for which results are available exhibiting sensitivity to some aspects of the design of the forecasting system. The primary aim is to show how the sensitivity studies provide indications of the importance of particular processes which are largely consistent with the theoretical and observational views discussed earlier. These cases also provide examples of some of the notable successes and failures of the ECMWF forecasting system, and evidence of past and likely future improvements to the system.

The cases to be discussed are divided for purposes of presentation into four categories. In the following section we present two quite different examples of orographic influences on cyclogenesis. Three cases of rapid development over eastern North America and the neighbouring Atlantic coastal region are then considered in Section 3. Further low-pressure systems of different types over the North Atlantic are discussed in section 4. This is followed by presentation of two cases of blocking, and a brief conclusion.

All results presented in this paper were obtained using variants of the global ECMWF spectral model; background information on the development of this model can be found in papers by Simmons and Jarraud (1984) and Simmons et al. (1988).

2. OROGRAPHIC INFLUENCES ON CYCLOGENESIS

a) Alpine lee cyclogenesis

The first example presented here is one of a direct beneficial impact of the horizontal resolution of the prediction model in a forecast of cyclogenesis in the lee of the Alps. It is drawn from a series of experimental forecasts which have been carried out at a resolution higher than the T106 resolution of the Centre's present operational model. The initial date of 20 March 1986 was

chosen because of an Alpine lee cyclogenesis early in the forecast range which was underestimated by the operational T106 forecast. A horizontal resolution of T159 was used, since it was the largest that could run efficiently within the memory constraints of the Centre's computer system, albeit over too long a time to be operationally practical. A one standard deviation envelope orography was adopted, and initial data were interpolated from the operational T106 analysis.

An improved prediction of the lee cyclogenesis was expected on the basis of the crudity of the representation of the Alps at lower spectral resolutions (e.g. Jarraud et al. 1986), and from results of Dell'Osso (1984) using different resolutions in a limited-area version of the ECMWF grid-point model. This was indeed found to be the case. Fig. 1 compares 1-day forecasts at T63, T106 and T159 resolutions with the verifying operational analysis. The superiority of T106 over T63 is evident, and T159 improves further over T106 in the intensity and shape of the lee cyclone. The T159 forecast shows detail which cannot be resolved in the T106 analysis used for verification, but the pressure and temperature fields exhibit patterns near the Alps and Pyrenees which are characteristic of high resolution hand analyses of similar synoptic situations, for example the cyclogeneses of the ALPEX period (e.g. Radinović, 1986).

A further experiment (not shown) confirms that it is the improved definition of the orography itself that gives rise to the forecast improvement shown in Fig. 1. Repeating the T106 forecast but with the T63 representation of orography results in a one-day forecast which is almost identical to the T63 forecast with respect to the lee cyclone. Beneficial impact of using envelope rather than mean orography for the representation of the Alpine barrier is discussed by Dell'Osso (1984) and Jarraud et al. (1986).

b) East Asian coastal cyclogenesis

A sensitivity of the prediction of cyclogenesis near the East Asian coast to the representation of model orography (mean or envelope) has been noted by Jarraud et al. (1986), and sensitivity was also found during the testing of the gravity-wave drag parametrization (Miller and Palmer 1987) now included in the operational ECMWF model. The case chosen to illustrate this is one in which the then-operational (T106, envelope-orography, no gravity-wave drag)

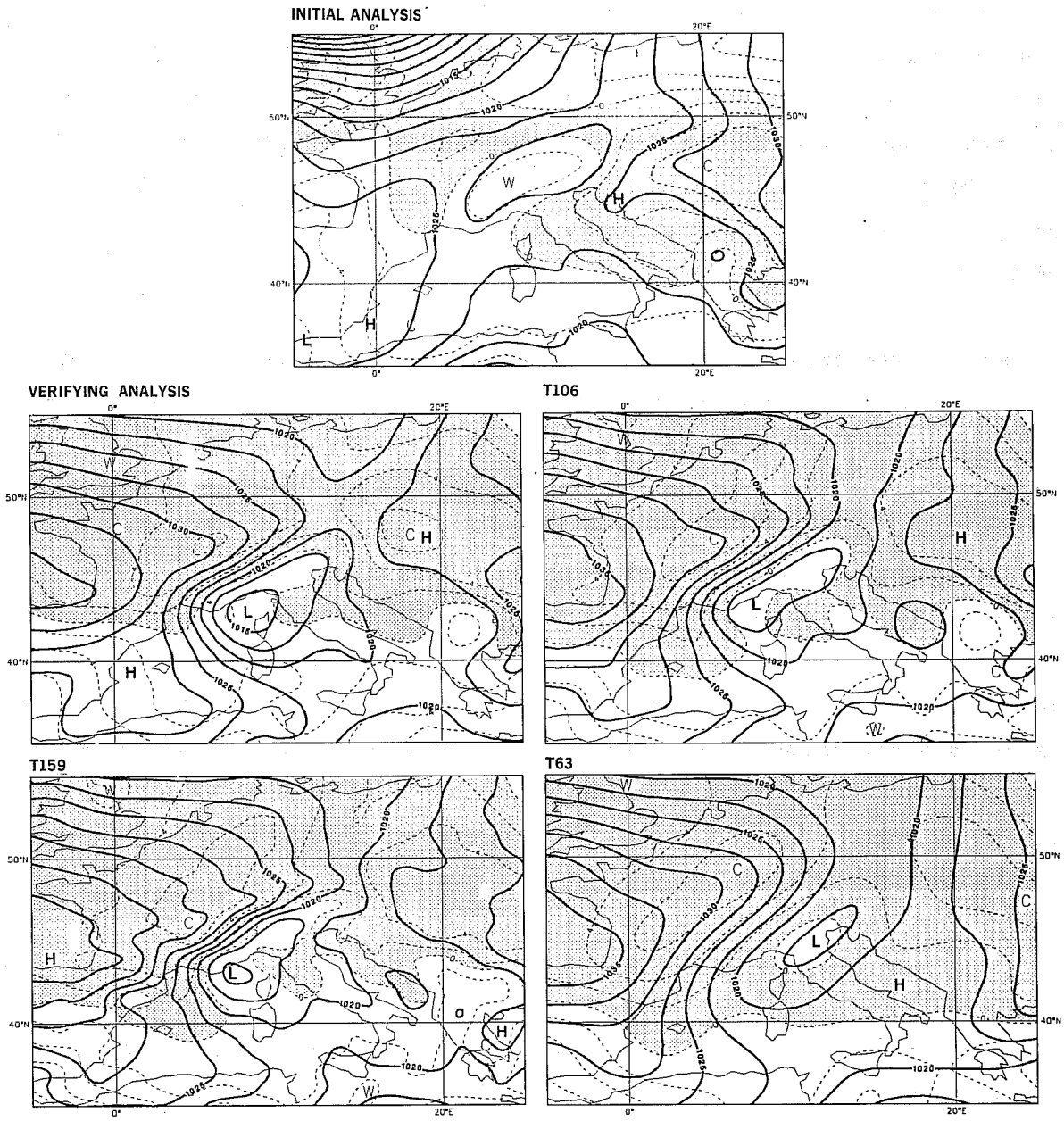

Fig. 1 The (T106) analysis for 12Z, 20 March 1986 (upper) and for 12Z, 21 March 1986 (middle left) and 1-day forecasts valid at the latter time performed using horizontal resolutions T106 (middle right), T159 (lower left) and T63 (lower right). Solid lines show mean sea-level pressure with a contour interval of 2.5 hPa, and 850 hPa temperature is denoted by dashed contours, with 2K interval, and by shading where values are below 0°C.

forecast produced a spurious explosive deepening in the medium range. Analyses of mean sea-level pressure over eastern Asia and the northwest Pacific are shown in the left-hand panels of Fig. 2 for 12Z on 20, 21 and 22 January 1986, and corresponding 5-, 6- and 7-day forecasts from 15 January are shown in the right-hand panels. Although some cyclone development happens in reality, it occurs with neither the intensity nor the spatial scale that is present in the forecast.

Four different 6-day forecasts are presented in Fig. 3. The upper-left map simply repeats the operational, envelope-orography forecast shown in Fig. 2, and this forecast is to be compared with forecasts produced using mean orography (upper right), envelope orography plus a parametrization of gravity-wave drag (lower left) and mean orography plus gravity-wave drag (lower right). The forecast with mean orography and no wave drag produces an even more rapid cyclone growth, while there is a much weaker, and smaller-scale development in the two forecasts which include the parametrization of gravity-wave drag. The improvement brought about by the latter is thus larger in the case of mean orography, in agreement with the general finding of Miller and Palmer (1987).

A number of preceding contributions to this Seminar have discussed the important rôle that is often played by mobile upper-air troughs in the process of development of intense surface lows. Examining sequences of synoptic maps suggests that it is orographic influences on the evolution of such a trough over central Asia earlier in the forecast range which are primarily responsible for the different development indicated in Fig. 3. To illustrate this, Fig. 4 presents 500 hPa height fields over Asia corresponding to days 2 and 4 of the forecast. The verifying analyses are shown in the upper panels, and corresponding forecasts with mean orography (middle) and with envelope orography plus gravity-wave drag (lower) are also shown. As early as day 2 small differences can be seen in the position of the trough marked in the figure, and in the ridge west of it. These differences become pronounced by day 4. In the analysis and forecast with envelope orography and gravity-wave drag there is a strong tilt to the trough, which is a weakening feature. Conversely, in the forecast with mean orography the trough is well established as a pronounced, eastward-moving feature, and rapid cyclone development occurs as it moves beyond the continental coastline. With envelope orography but no

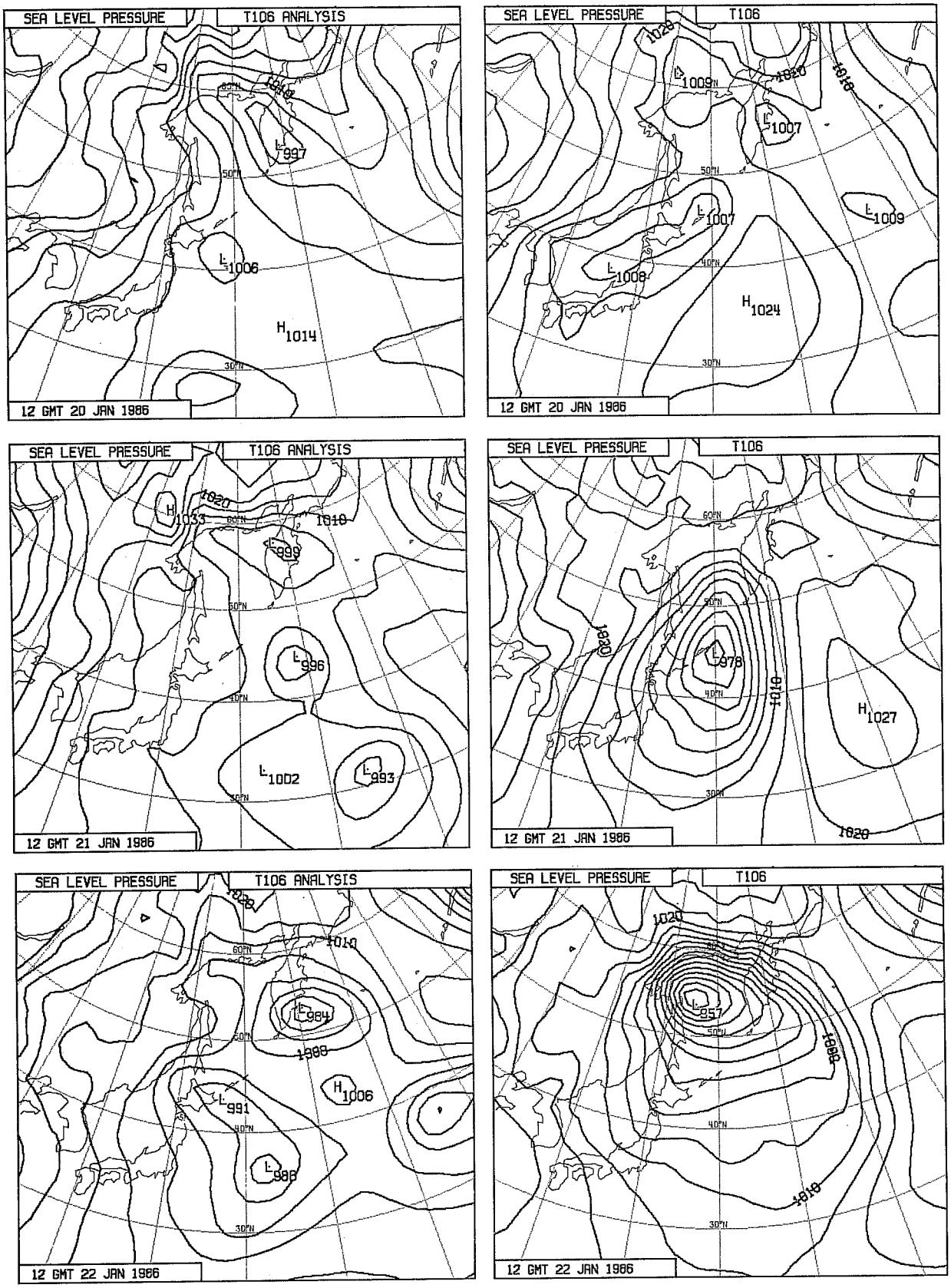

Fig. 2 Analyzed maps of mean sea-level pressure (contour interval 5hPa) for 12Z 20 January (upper left), 21 January (middle left) and 22 January (lower left), 1986. Corresponding 5-, 6- and 7-day forecasts from 15 January 1986 are plotted on the right-hand side.

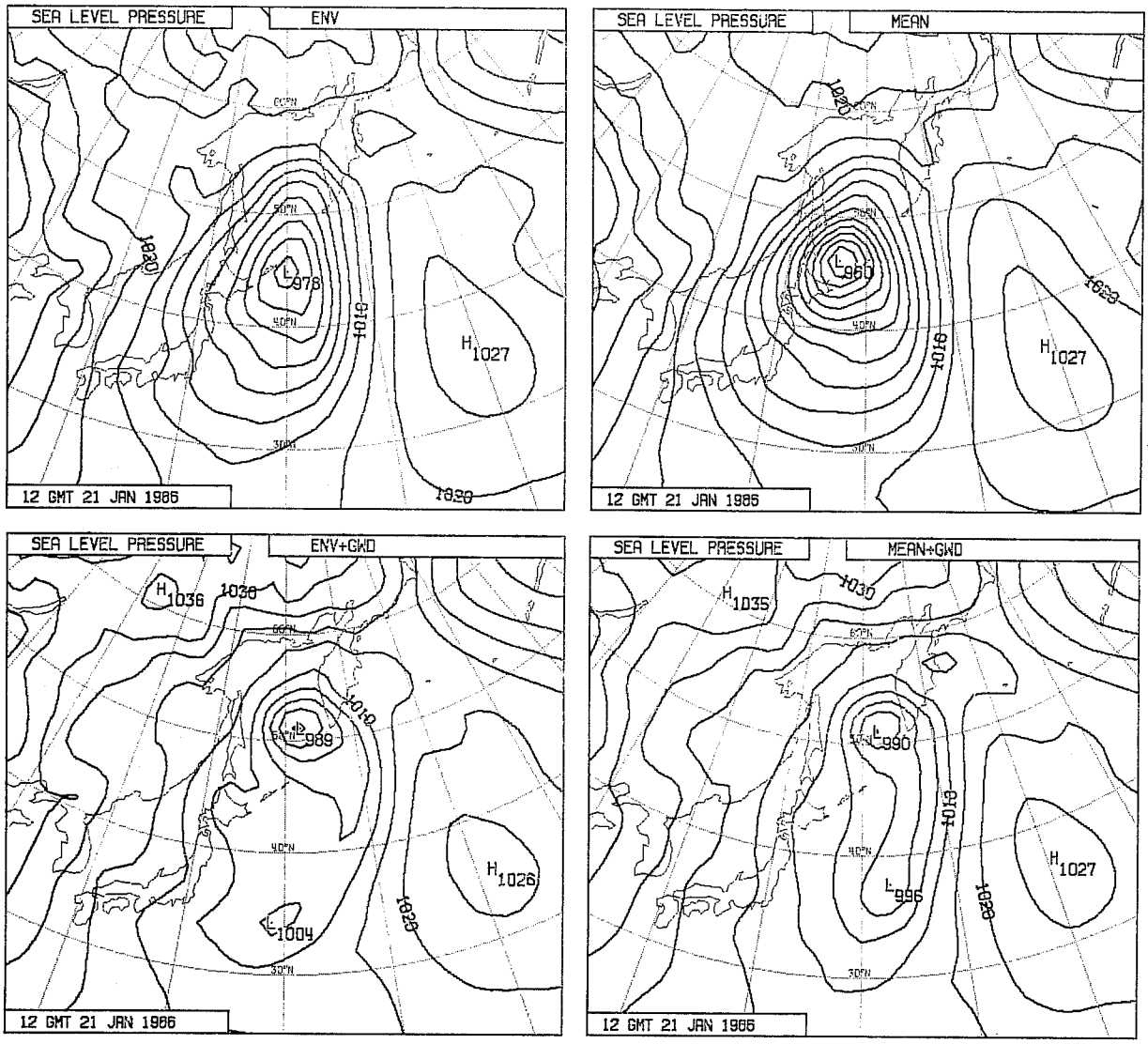

Fig. 3 Four 6-day forecasts of mean sea-level pressure (contour interval 5hPa) verifying at 12Z, 21 January 1986
Upper left: Envelope orography, no gravity-wave drag
Upper right: Mean orography, no gravity-wave drag
Lower left: Envelope orography, gravity-wave drag
Lower right: Mean orography, gravity-wave drag

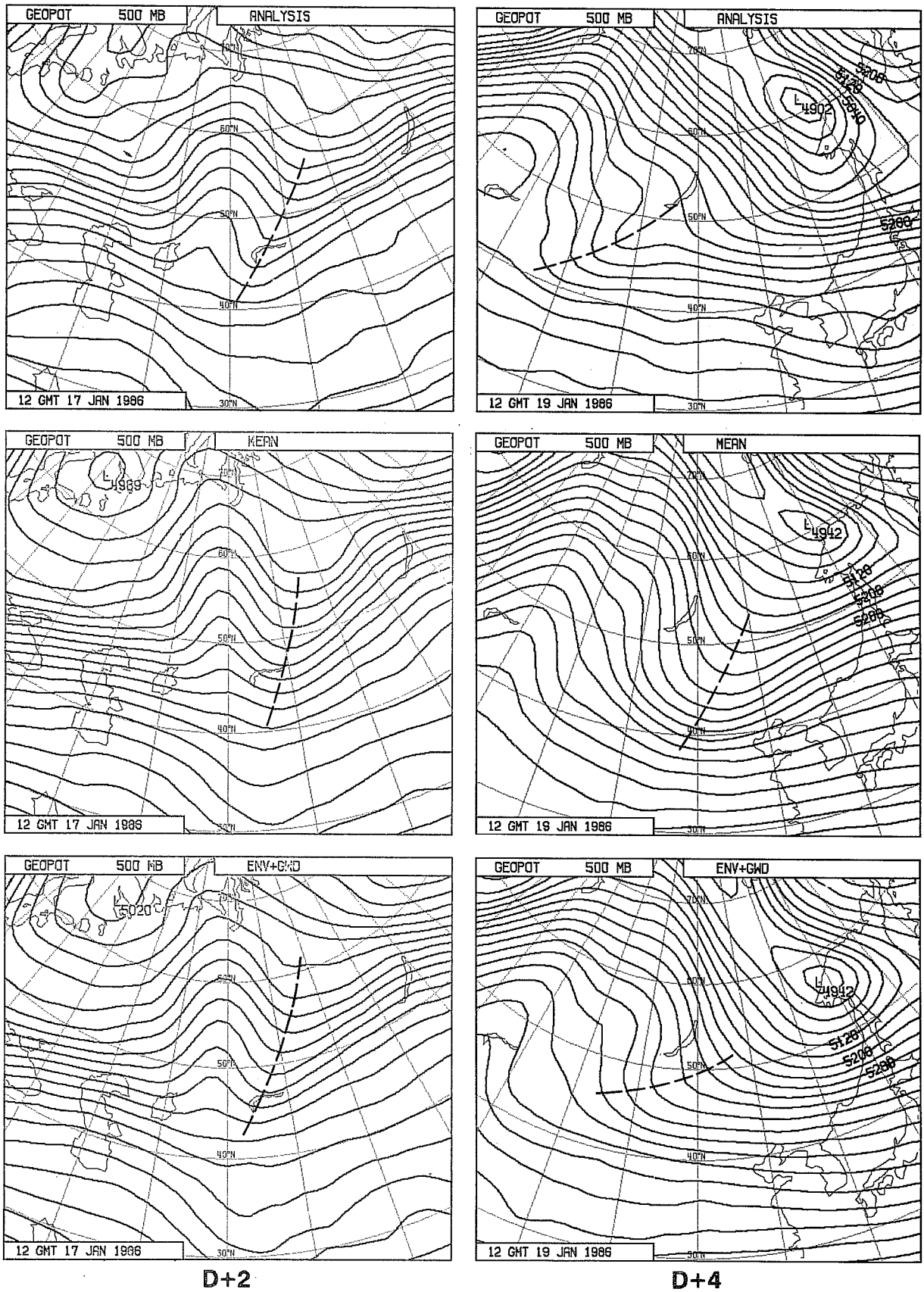

Fig. 4 Analyses (upper) and forecasts using mean orography and no gravity-wave drag (middle) and envelope orography and gravity-wave drag (lower) for the 500 hPa height field (contour interval 60m) at 12Z, 17 January (left) and 19 January (right) 1986. The initial date for the forecasts was 15 January.

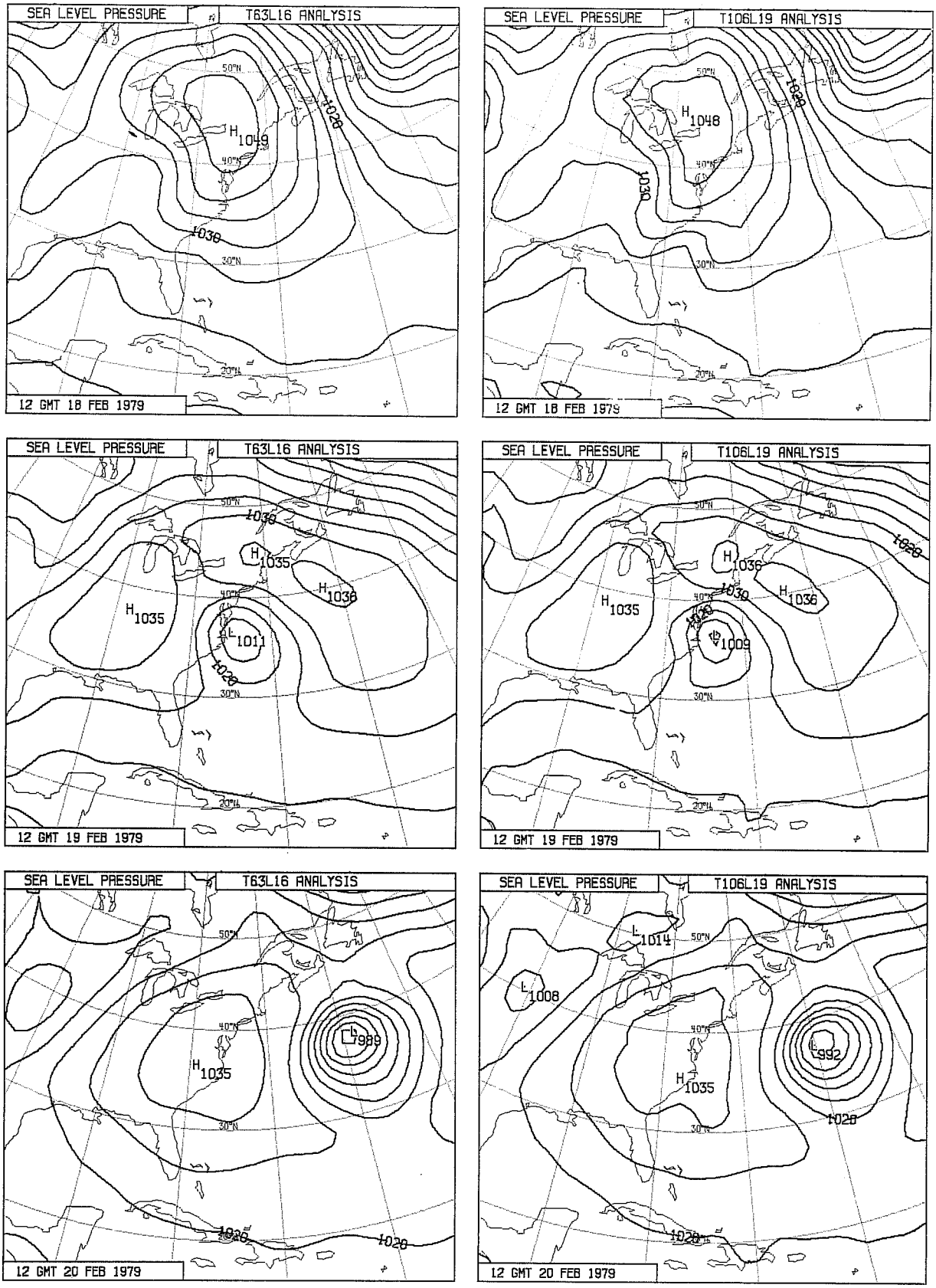

Fig. 5 T63L16 (left) and T106L19 (right) analyses of mean sea-level pressure (contour interval 5hPa) for 12Z, 18 February (upper), 19 February (middle) and 20 February (lower) 1979.

parametrization of gravity-wave drag the trough moves eastward much as in the mean orography case, but with rather less amplitude, consistent with the lower intensity of the subsequent surface development.

3. RAPID DEVELOPMENT OVER EASTERN NORTH AMERICA AND THE WESTERN ATLANTIC

a) The Presidents' Day Storm

Uccellini, in these Proceedings, has discussed the evolution of the Presidents' Day Storm of February 1979. Although from a date prior to the start of routine forecasting at ECMWF, this case has been studied as part of the Centre's use of FGGE data, and several points of interest arise from the performance of the ECMWF forecasting system for this situation.

The results presented here are derived from two different assimilations of the observational data. The first is the so-called "Final III-b" assimilation. The assimilating model in this case used the T63 16-level resolution of the original version of the spectral model, and mean orography. The resulting analyses will be referred to as T63L16. The second assimilation used the same set of observational data, but the revised data analysis system introduced operationally in September 1986. The assimilating model in this case used the current operational 19-level T106 (T106L19) resolution and envelope orography.

A comparison of the two sets of surface pressure analyses, for 12Z on 18, 19 and 20 February 1979, is presented in Fig. 5. For 18 February, the T106L19 analysis exhibits a sharper tongue of high pressure east of the Appalachian Mountains, indicative of a more pronounced cold-air damming associated presumably with the higher horizontal resolution and envelope orography of the assimilating model. The inverted trough to the east is also a more prominent feature. The storm itself is seen to be 2 hPa deeper (though still not as intense as illustrated by Uccellini) in the T106L19 analysis for 19 February, although the converse is the case one day later. At this time an inverted trough off the East Coast can again be seen more clearly in the T106L19 analysis.

Maps of isentropic potential vorticity for the 310K surface are presented in Fig. 6 at 12 hourly intervals commencing 12Z, 17 February, for the T106L19 analysis. This figure illustrates the evolution of the upper-air trough that

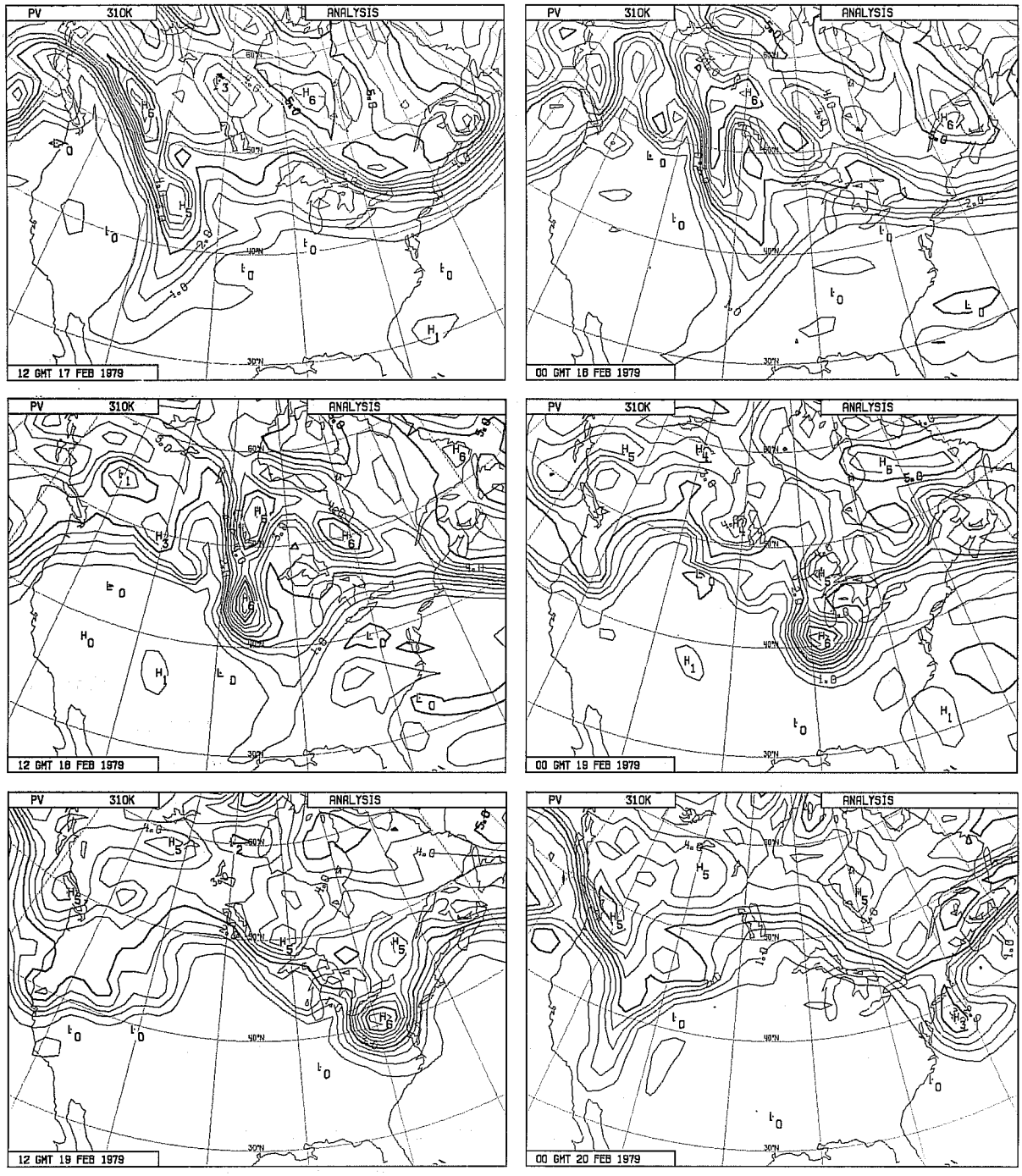

Fig. 6 Isentropic potential vorticity maps for the 310K surface at 12-hourly intervals from 12Z, 17 February to 0Z, 20 February 1979, for the T106L19 analysis. The unit is 10^{-6} $m^2s^{-1}K$ kg^{-1}, and the contour interval is 0.5.

appears to play a significant rôle in the development of the storm. Examining these maps, and corresponding plots for the intermediate 6 and 18Z analyses, reveals a strong degree of temporal continuity, with little change in the potential vorticity maximum until after 12Z on 19 February, when it was presumably altered by the diabatic processes active within the vicinity of the surface low. Comparison with Uccellini's plots for the 312 K surface reveals a high degree of consistency.

Forecast sensitivity experiments were initially carried out from 12Z 17 and 18 February, using the T63L16 analyses interpolated to allow for use of (one standard-deviation) envelope orography (for all experiments reported here) and higher resolution (for some experiments). Development was generally underestimated from these analyses. We present two sets of results of 2-day forecasts from 18 February. Similar results, though with weaker development, were obtained from the earlier time.

The impact of resolution is illustrated in Fig. 7. Increasing the horizontal resolution from T63 (upper right panel) to T106 (lower left) improves the depth of the low, although it remains weaker than observed. Using T63 horizontal resolution but a 31-level vertical resolution in which layer thicknesses are approximately halved above the planetary boundary layer, gives rise to a slightly larger improvement at the surface (lower right panel), and also a better-defined upper-air trough (not shown).

Repeating the T106 forecast, but with the operational Kuo convection scheme replaced by the adjustment scheme of Betts and Miller (1986), results in a further (and larger) improvement in the intensity of the storm, as illustrated in Fig. 8. This figure also includes the result of an integration in which latent heating was suppressed. The absence of development is conspicuous for this latter integration.

The most dramatic sensitivity found in this case is to the choice of initial analyses. Forecasts from the T106L19 analyses for 12Z, 17 and 18 February both produced development of about the observed intensity. The two- and three-day forecasts from 17 February are compared with the corresponding T106 forecasts from the T63L16 analysis in Fig. 9, and the substantial improvement in the forecast is evident. The integration from the T106L19 analysis used a

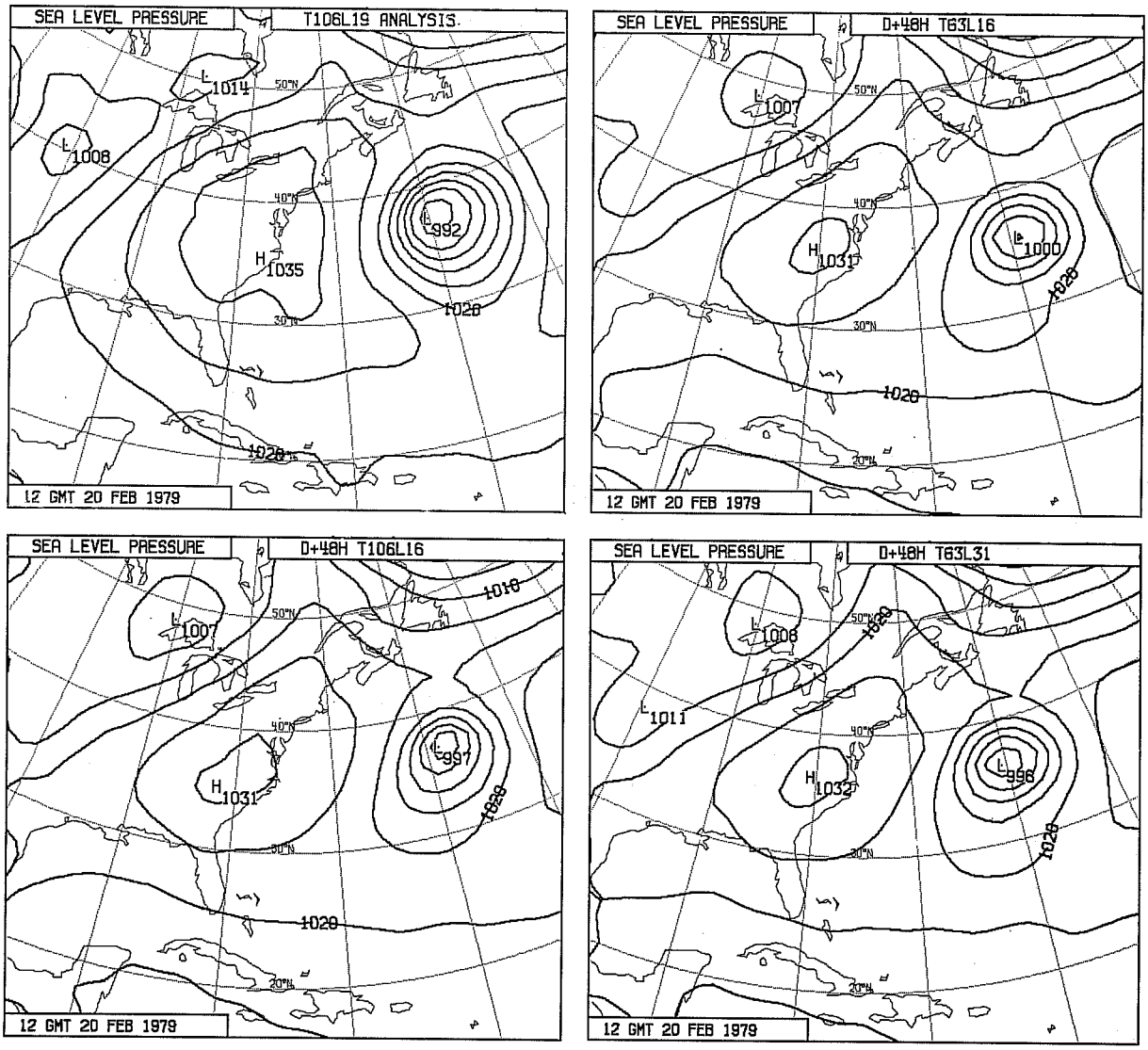

Fig. 7 The (T106L19) mean sea-level pressure analysis (contour interval 5hPa) for 12Z, 20 February 1979 (upper left) and 48-hour forecasts verifying at this time with
Upper right: T63, 16-level resolution
Lower left: T106, 16-level resolution
Lower right: T63, 19-level resolution.

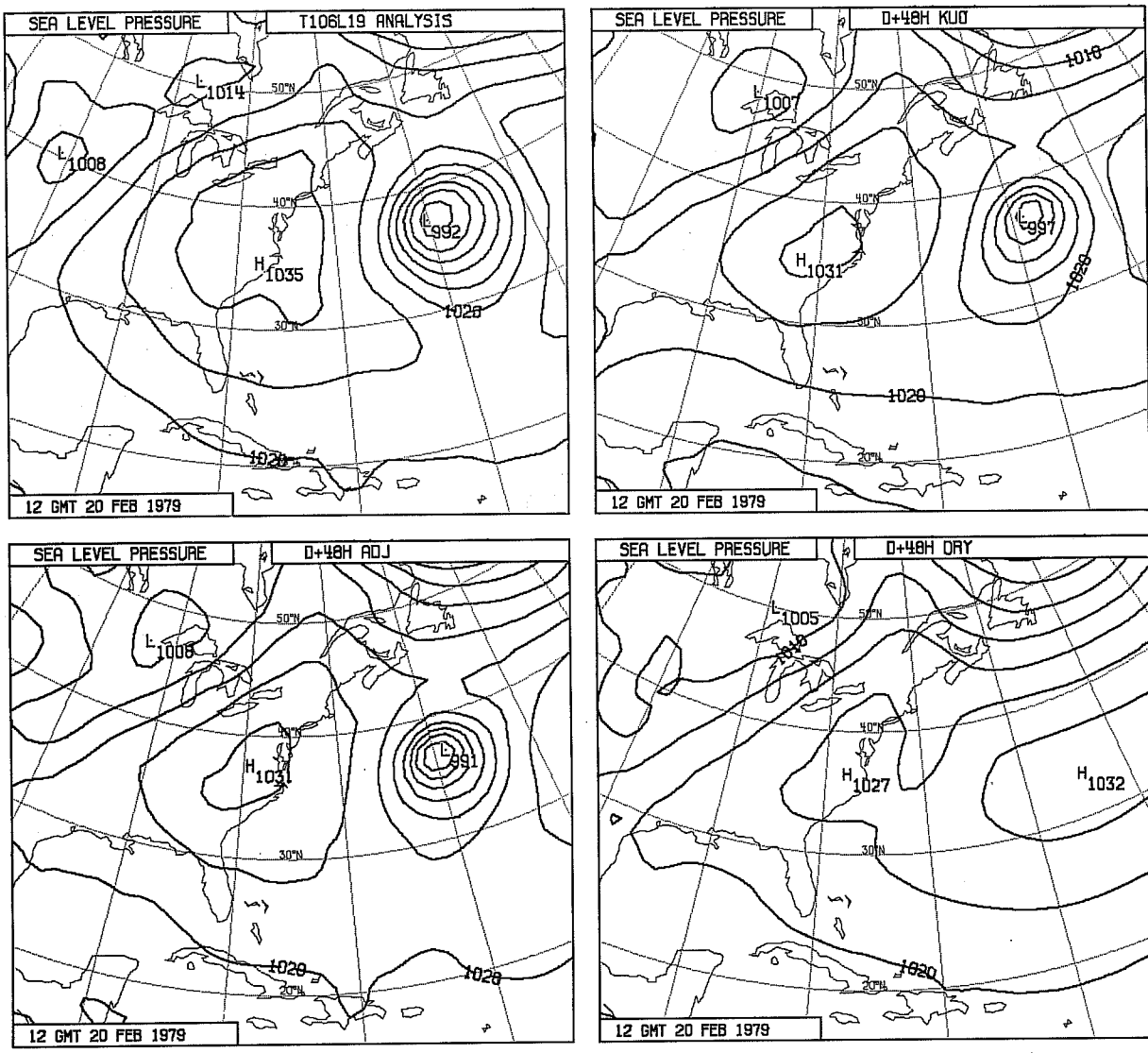

Fig. 8 The (T106L19) mean sea-level pressure analysis (contour interval 5hPa) for 12Z, 20 February 1979 (upper left) and 48-hour forecasts verifying at this time with
Upper right: Kuo convection scheme
Lower left: Betts-Miller convection scheme
Lower right: Suppression of moist processes

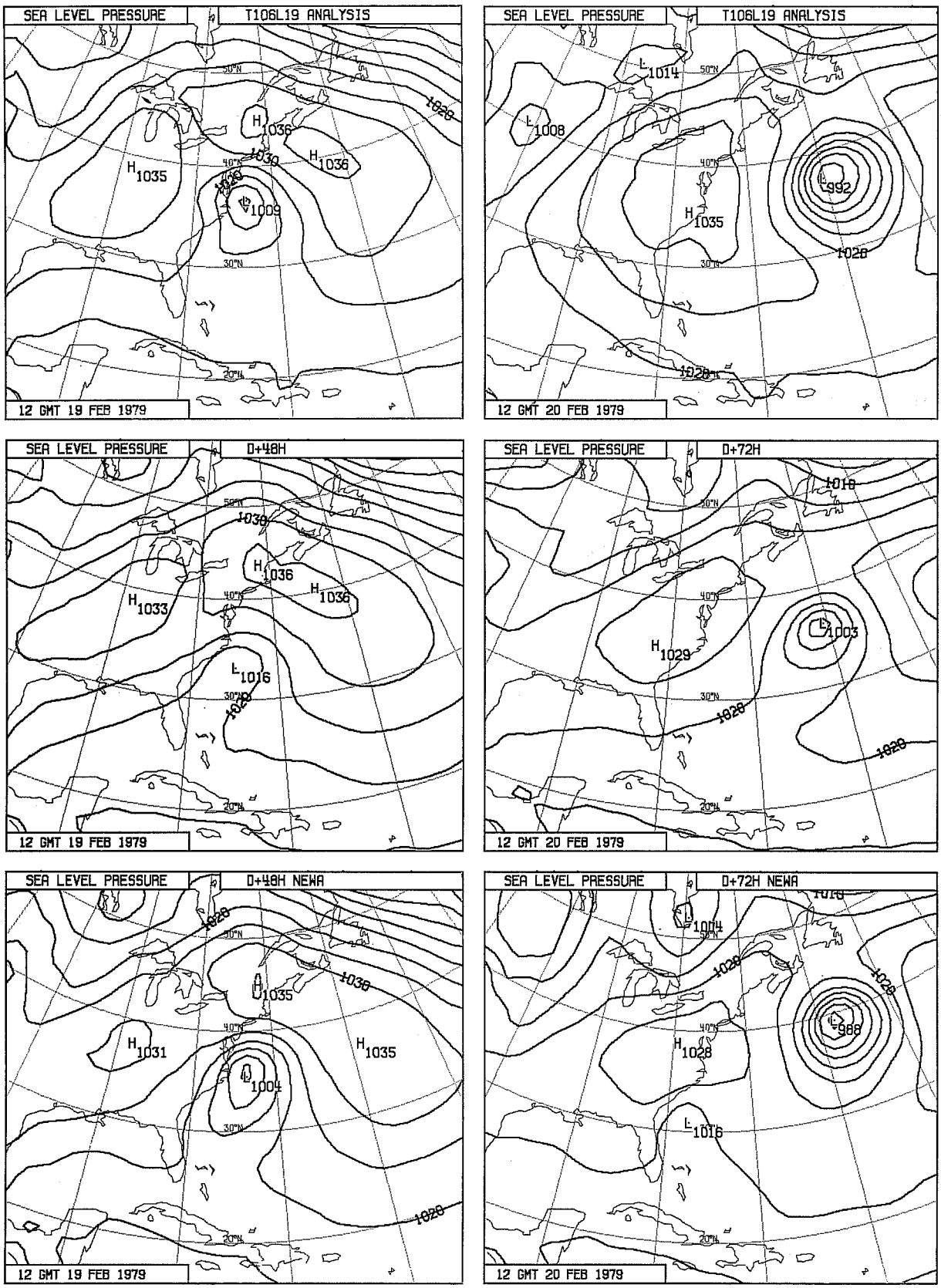

Fig. 9 T106L19 mean sea-level pressure analyses (contour interval 5hPa) for 12Z, 19 February (upper left) and 20 February (upper right), together with 48-hour (left) and 72-hour (right) forecasts from 17 February using the T63L16 analysis (middle) and the T106L19 analysis (lower).

newer version of the model than did that from the T63L16 analysis, but separate experiments have shown the changes to have negligible impact on the forecasts of interest. We have not attempted to identify the extent to which the improvement shown in Fig. 9 result from the change in analysis code or from the use of a higher resolution model in the assimilation, but it is gratifying that the current operational assimilation system has performed so much better in this case.

It is necessary, however, to introduce a note of caution, in that forecasts from both analyses exhibit a tendency to lose amplitude in the upper-air trough. Fig. 10 presents isentropic potential vorticity maps for the 310K surface for the two analyses for 12Z, 17 February, and for one- and two-day T106 forecasts from these analyses. The higher resolution of the T106L19 analysis is clearly seen in the maps for 17 February, and the larger maximum in potential vorticity over the Canadian Rockies present in this analysis is reflected in a larger maximum in the corresponding forecast as the trough moves towards the eastern seaboard. Nevertheless, a decrease in the maximum is evident in the forecasts from both analyses, in contrast with the quite uniform maximum value seen in Fig. 7 for the analyses over this period.

The above finding led us to use this case as one for examining the impact of reducing the parametrized vertical diffusion in the free atmosphere. Such a change was under investigation as a result of other diagnostic studies, and has recently been implemented operationally. The impact of the change in the case of the Presidents' Day Storm is to enhance development, particularly in the forecasts from the T63L16 analyses, as illustrated in Fig. 11. However, this enhancement takes place despite there being little impact on the reduction in the potential vorticity maximum, as can also be seen in Fig. 11.

Overall, the sensitivities seen in these forecast experiments are much as could be expected from our understanding of the storm as derived from work such as that presented by Uccellini. It is clear that with such a variety of ways of improving this particular forecast, undue emphasis should not be placed on the beneficial impact of any particular change. The apparent inability to maintain the amplitude of the potential vorticity maximum associated with the upper-air trough remains a cause for concern and future investigation.

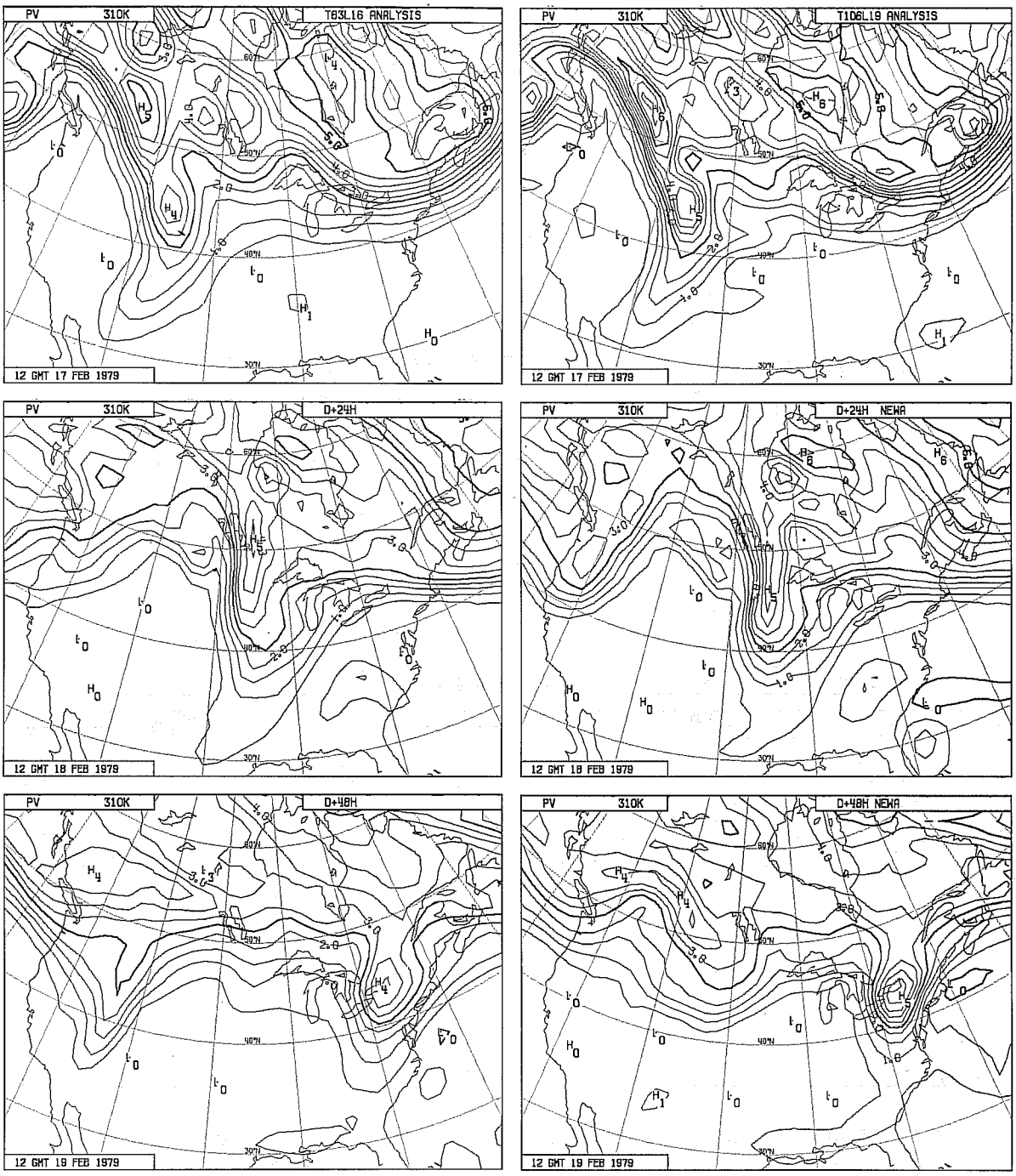

Fig. 10 Isentropic potential vorticity maps for the 310K surface, with units as in Fig. 6. The T63L16 and T106L19 analyses for 12Z 17 February 1979 are shown (left and right, respectively) in the upper panels, and 24- and 48-hour forecasts from these analyses are shown in the middle and lower panels.

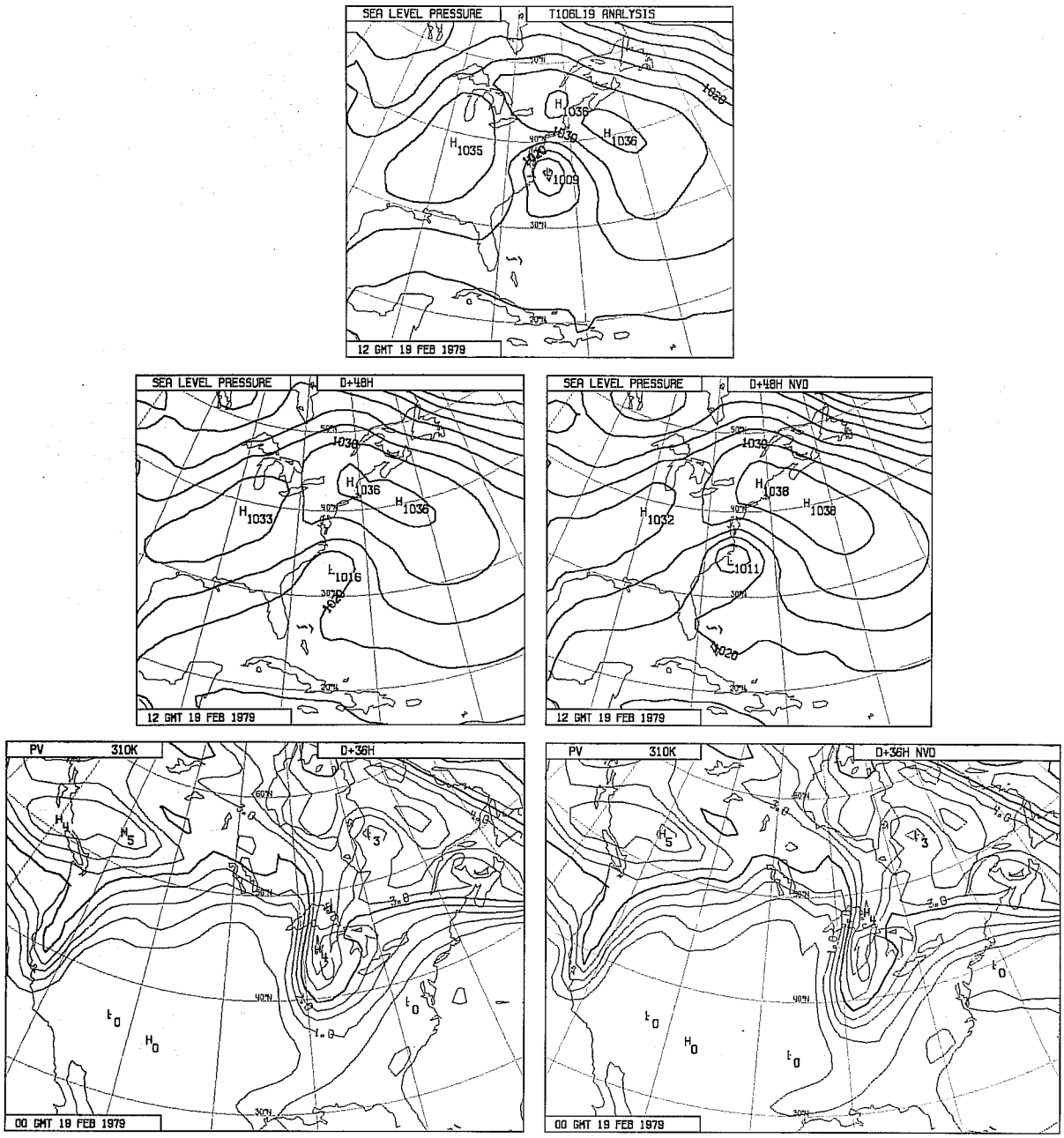

Fig. 11 The T106L19 mean sea-level pressure analysis (contour interval 5hPa) for 12Z, 19 February 1979 (upper) and 48-hour forecasts valid at this time from the standard model (middle left) and with reduced vertical diffusion (middle right). The potential vorticity maps for the 310K surface from the 36-hour forecasts are shown in the lower panels.

b) The Cleveland Storm of January 1978

This case involves the rapid development of an extreme storm (with minimum surface pressure centred over Cleveland, Ohio) associated with the "phasing" of troughs in the northern and southern branches of the westerlies (Wagner, 1978; Bosart, personal communication). A spell of data assimilation has been carried out for a period prior to and during the development and early decay of the storm, using observational data gathered as part of preparatory work for the FGGE observing year. Forecast experiments are being carried out.

Maps of 500 hPa height and sea-level pressure are presented in Fig. 12 for the analyses for 12Z on 24, 25 and 26 January, 1978. The upper-air maps for the first two days show the southeastward movement of a low over Canada, and the eastward movement of a second low over the southern United States. These come into close conjunction during the 24 hours following 12Z on 25 January, and over this period there is the development of a surface low of remarkable depth and spatial scale, and complex frontal structure.

Sea-level pressure maps are presented in Fig. 13 for 48- and 54-hour forecasts for 12Z and 18Z, 26 January, around the time of peak intensity, together with the verifying analyses. The latter are shown in the upper panels. The middle panels show the forecasts produced using the operational ECMWF model as of summer, 1987, while the lower panels show results obtained with a reduction in parametrized vertical diffusion in the free atmosphere. As shown for the Presidents' Day storm, and found for other cases of rapid cyclogenesis, deeper (and more realistic) development is found with the revised parametrization.

The availability of a set of analyses using a current data assimilation system, and the capability for making an accurate numerical forecast, provides the basis for future study of the nature of this major storm. It is beyond the scope of the present paper to go much further, but it is of interest to look at analyzed and forecast maps of isentropic potential vorticity. These are shown in Fig. 14 for 18Z, 25 January and for 6 and 18Z, 26 January, the forecast being from 12Z, 24 January (with reduced vertical diffusion). Analysis and forecast are in reasonable agreement, exhibiting a decay of the maximum associated with the southern trough, and a striking wrapping round of regions of high and low potential vorticity. Negative potential vortiticies occur in both analysis and forecast near Lake Superior; the realism and relevance of these is a matter for further investigation.

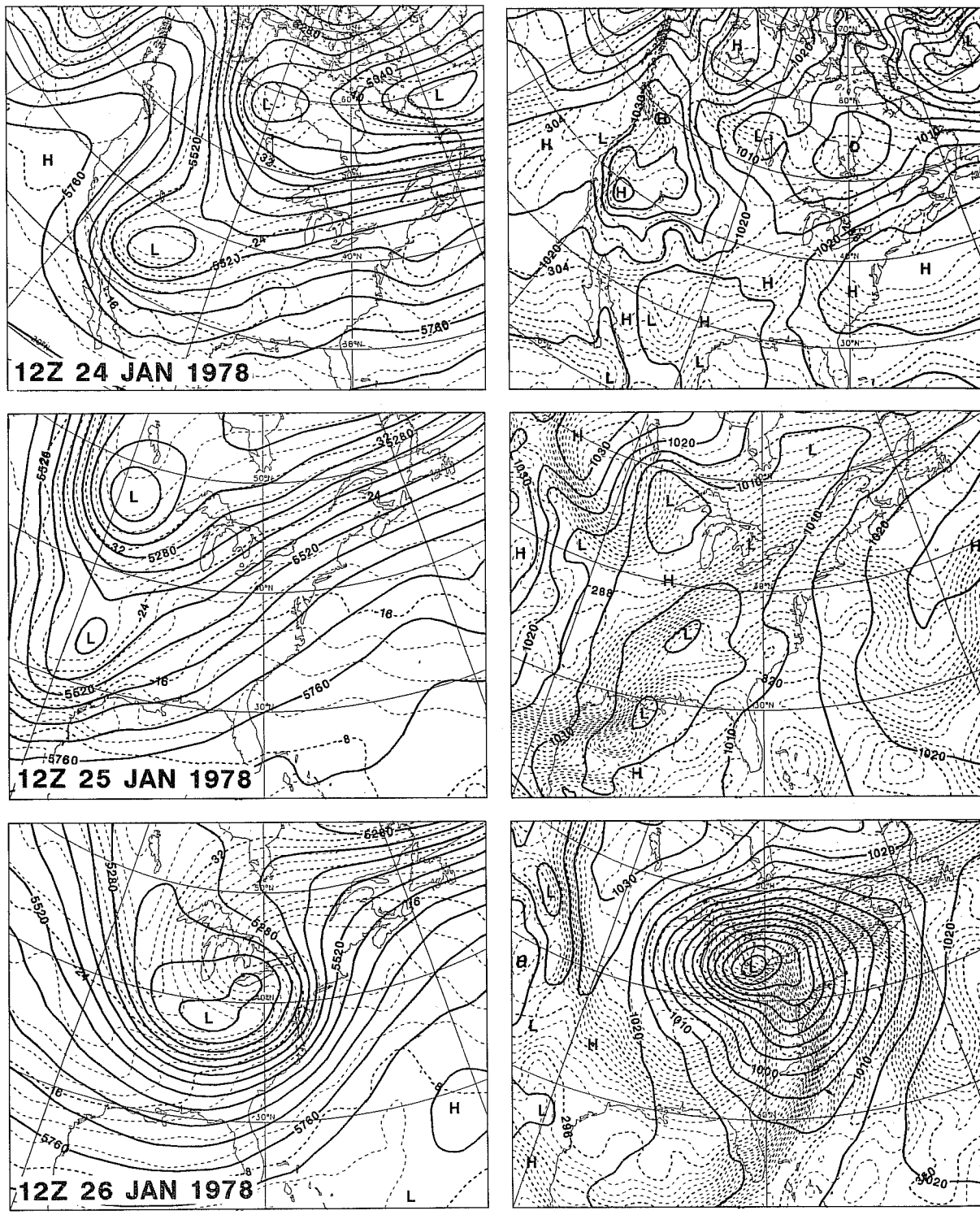

Fig. 12 Analyses of 500hPa height and temperature (contour intervals 60m and 2K, shown left) and of mean sea-level pressure and 850 hPa equivalent potential temperature (intervals 5hPa and 2K, right) for 12Z, 24 January (upper), 25 January (middle) and 26 January (lower), 1978.

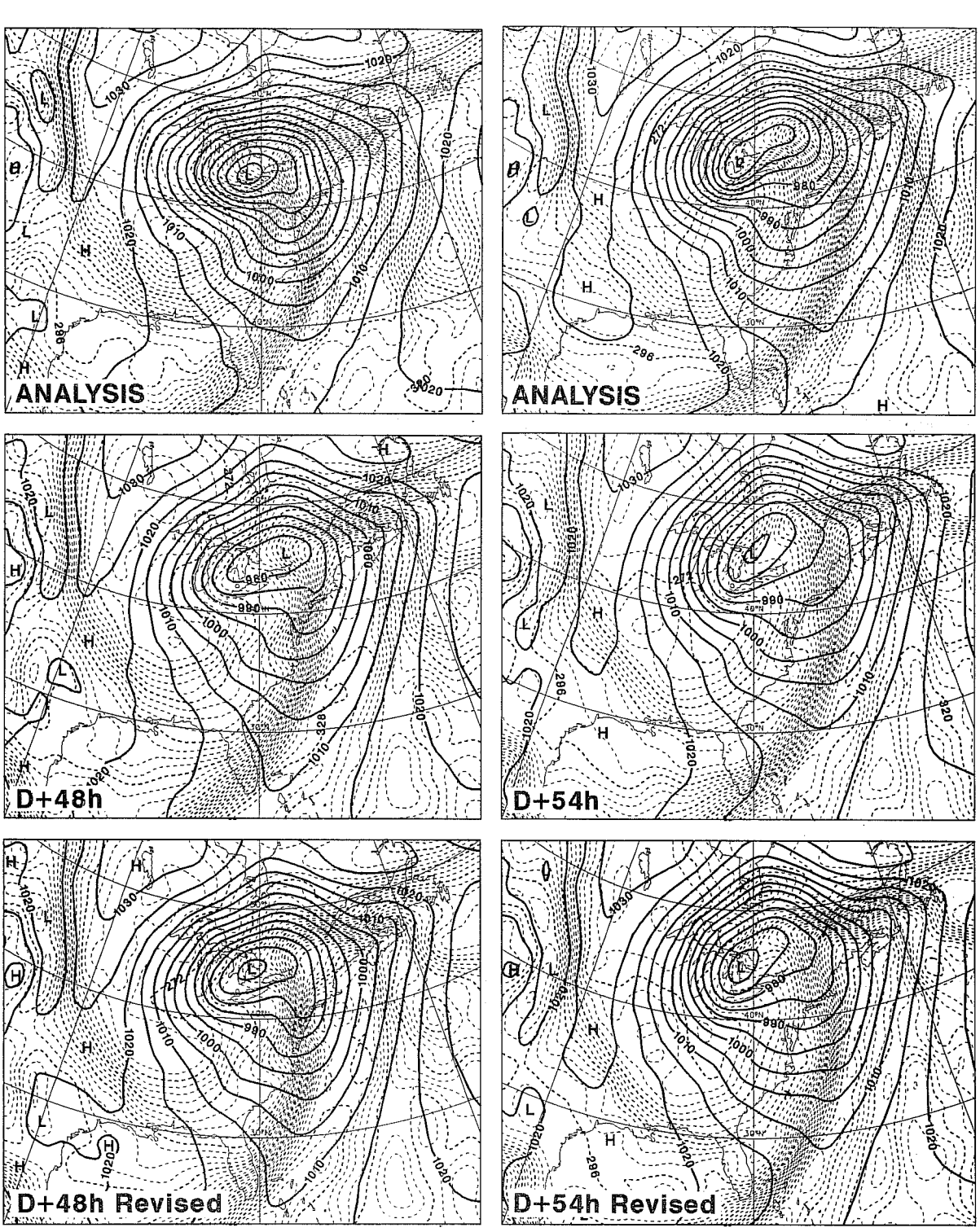

Fig. 13 Mean sea-level pressure (contour interval 5hPa) and 850hPa equivalent potential temperature (interval 2K) for 12Z (left) and 18Z (right), 26 January 1978:
Upper: Verifying analyses
Middle: 48- and 54-hour forecasts with standard model
Lower: 48- and 54-hour forecasts with reduced vertical diffusion.

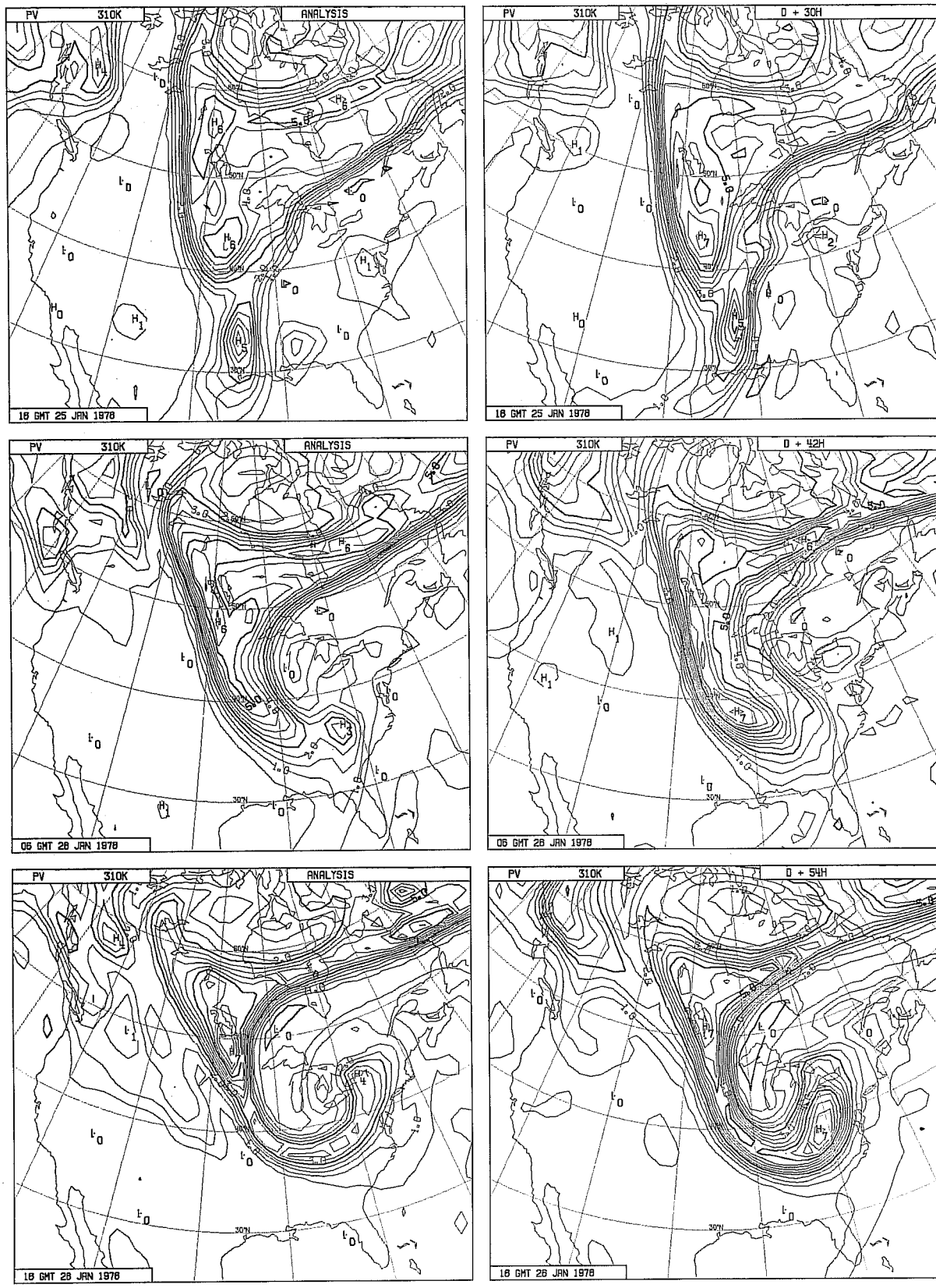

Fig. 14 Isentropic potential vorticity maps for the 310K surface, with units as in Fig. 6. The left-hand panels show analyses for 18Z, 25 January (upper) and for 6Z (middle) and 18Z (lower), 26 January 1978. The right-hand panels show corresponding 30-, 42- and 54-hour forecasts from 12Z, 24 January.

c) A recent failure

To contrast the successful forecasts at two-day range illustrated in the preceding two examples, a recent striking failure in a rather similar case of cyclogenesis is now noted. The case has been chosen independently for discussion by Bosart in these Proceedings, and Fig. 15 repeats analyzed maps of 500 hPa height and sea-level pressure for 12Z, 23 February 1987 and corresponding maps from the 48-hour forecast for this time. There is evidently a substantial error in the intensity and position of the surface low which in reality gave significant snowfall over the East Coast of the United States.

The evolution of this storm is also associated with the phasing of two troughs upstream of the region of surface development. The initial 500 hPa height field for the forecast is shown in the upper panel of Fig. 16. The troughs in question are located over central Canada and the vicinity of the US/Mexico border. The other maps in Fig. 16 show 500 hPa height analyses and forecasts for 24 and 36 hours later. The analysis maps illustrate how the northern trough moves south eastwards while the southern trough moves rapidly to the northeast, so that the two come into phase by 0Z, 23 February. The northern trough is treated quite accurately by the forecast, but there is a substantial underestimation of the movement of the southern trough, which presumably accounts for the lack of subsequent surface development. As the phase error is apparent once the trough has crossed the southern Rockies, there is a possibility that misrepresentation of orographic effects plays a significant rôle.

4. DIFFERENT TYPES OF LOW-PRESSURE SYSTEM OVER THE NORTH ATLANTIC

a) Rapid cyclogenesis

A case of rapid cyclogenesis over the central North Atlantic is illustrated in Fig. 17. The upper plots show analysed surface pressures for 12Z on 12 and 13 January 1986, indicating a deepening of 50 hPa over the 24-hour period. This deepening was accurately captured by the 24-hour operational forecast from 12 January, which is shown lower right. In contrast to the case of the Presidents' Day storm shown earlier, there is still significant development when moist processes are suppressed (lower left), although latent heating accounts for some 20 hPa of the deepening.

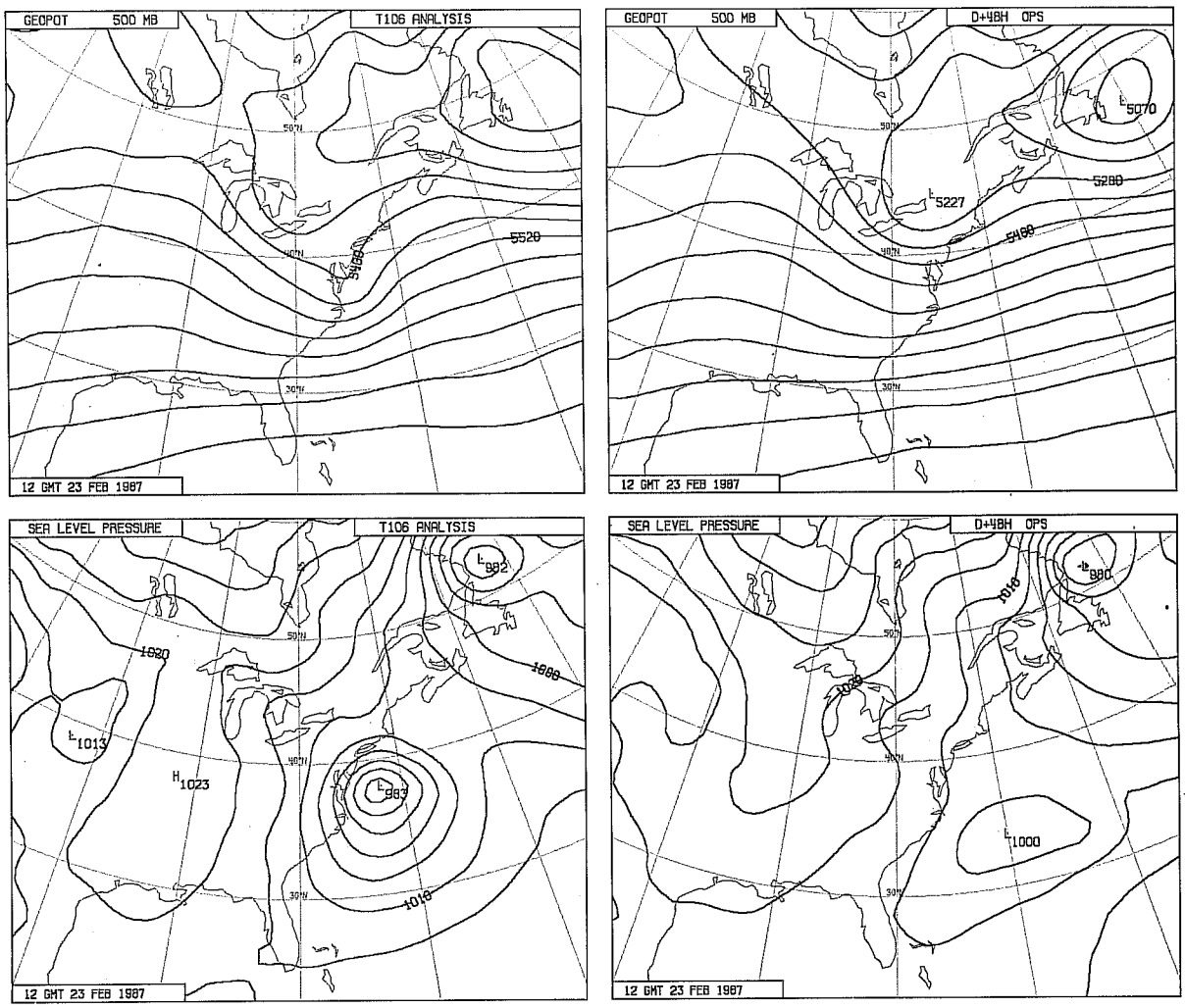

Fig. 15 500 hPa height (upper, contour interval 60m) and mean sea-level pressure (lower, interval 5hPa) for 12Z, 23 February 1987. The operational analysis is shown left, and the 48-hour operational forecast valid at this time is shown right.

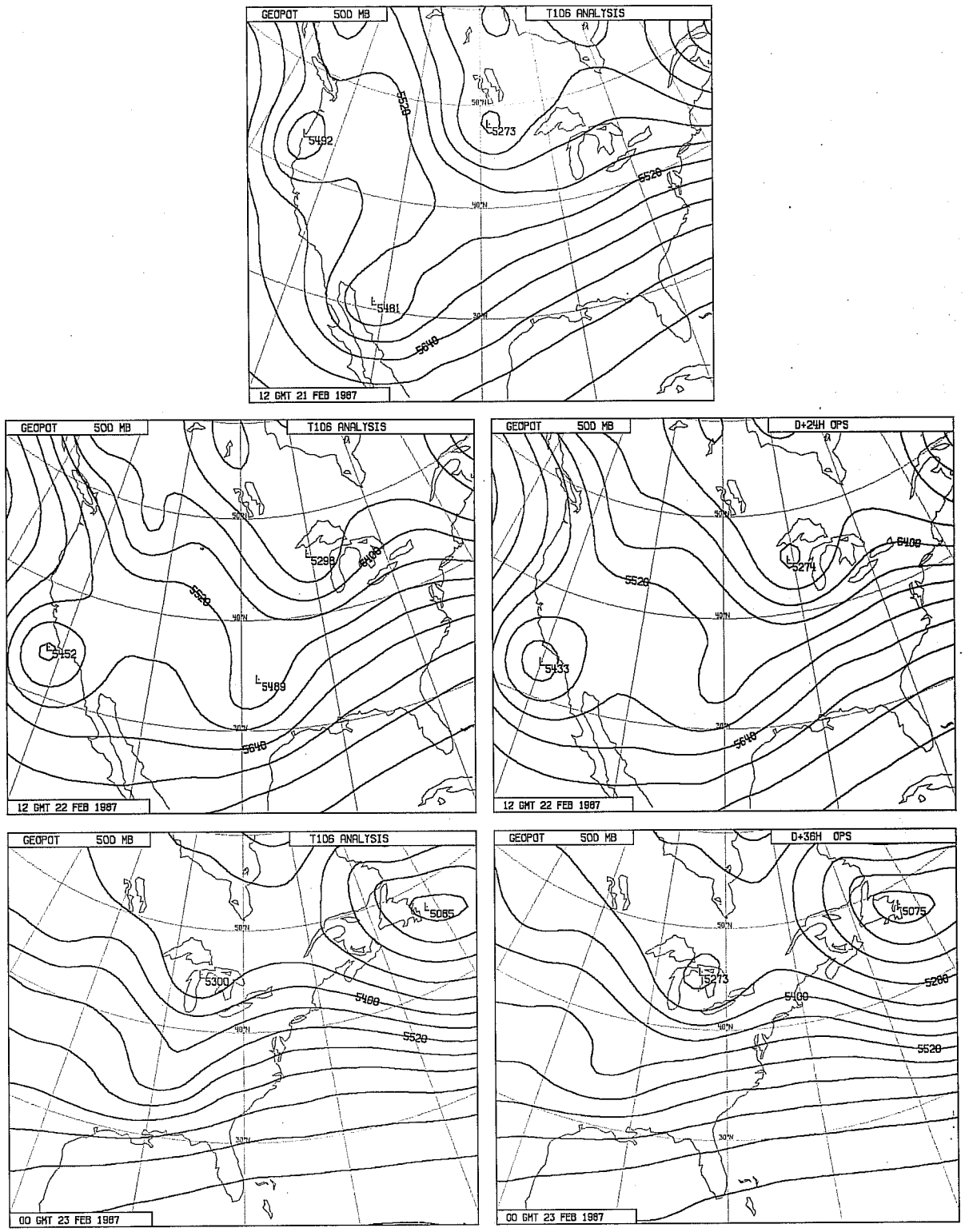

Fig. 16 Analysed 500 hPa height (contour interval 60m) for 12Z, 21 February (upper) and 22 February (middle left) and for OZ, 23 February (lower left), 1987. The middle and lower right-hand panels show 24- and 36-hour forecasts from 21 February.

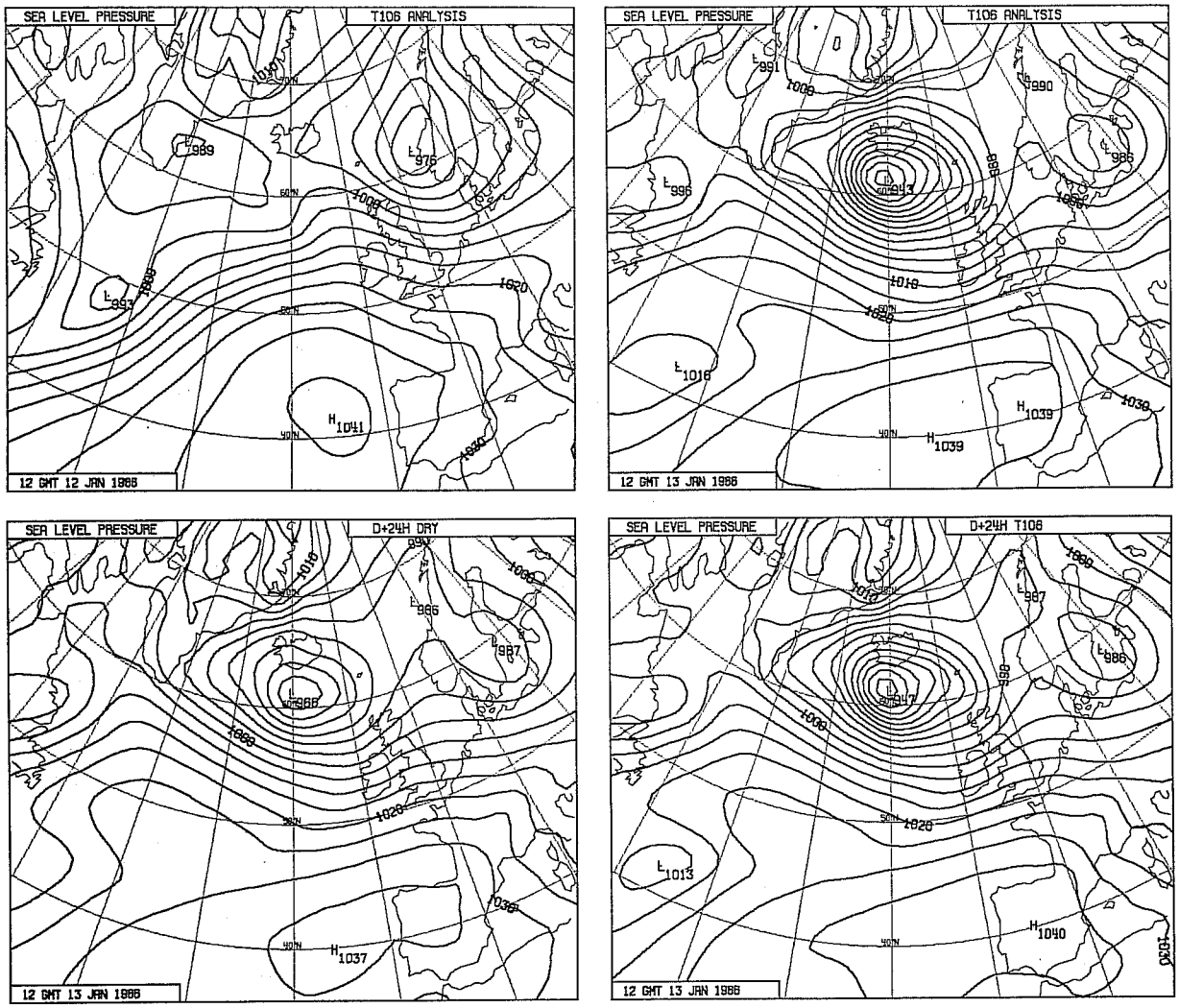

Fig. 17 Mean sea-level pressure (contour interval 5hPa) analysed for 12Z, 12 January (upper left) and 13 January (upper right) 1986. The operational 24-hour forecast from 12Z, 12 January is shown lower right, and the corresponding forecast with moist processes suppressed is shown lower left.

The sensitivity of the 24-hour development to the horizontal resolution of the forecast model has also been examined in this case, and T63, T106 and T159 forecasts are compared in Fig. 18. The overall rapid growth of the system is clearly captured quite well by all resolutions at this short forecast range, although extensive comparisons of T63 and T106 have identified the resolution increase as being generally beneficial for the prediction of the deepening and tracking of depression over the Atlantic and Pacific Oceans (e.g. Simmons et al., 1988). In the present case the increase of resolution from T63 to T106 and then from T106 to T159 results in increases of intensity of several hPa, the depth of the low being captured most accurately with T159. It is more difficult to verify differences in thermodynamic structure between T159 and T106 because of the bias of the verifying analysis towards the T106 resolution, but the waviness of the cold front at T63 resolution disagrees with the analysis, with the higher resolution forecasts and with satellite imagery. Some of this waviness can also be seen in the T106 forecast, and the occlusion is less advanced and well-defined (and less in agreement with observation) at this resolution than at T159.

Our attention in many examples in this paper is firmly focused on the performance of the forecasting system at quite short ranges. Understanding the successes and failures of the system in the short-range, when there has been less time for the complicating interaction of different errors, provides a basis for improvements which can be expected to lead to benefit across the whole forecast range. Nevertheless, it is appropriate here to remind ourselves of the primary goal of ECMWF, the improvement of the medium-range forecast, and examine how the deep Atlantic low of 13 January was captured by earlier forecasts.

Fig. 19 thus shows maps of sea-level pressure for operational forecasts verifying at 12Z on 13 January at ranges from one to six days. Viewed from a hemispheric perspective all could be regarded as successful in some sense, in that each has produced a surface-pressure minimum below 970 hPa in the vicinity of Iceland. Looking more locally, the front approaching Ireland and westerly flow over the United Kingdom are captured quite well up to five days in advance. However, for the purposes of predicting the wind speed and direction over the waters immediately south of Iceland, the forecasts must be regarded as poor from day 3 onwards.

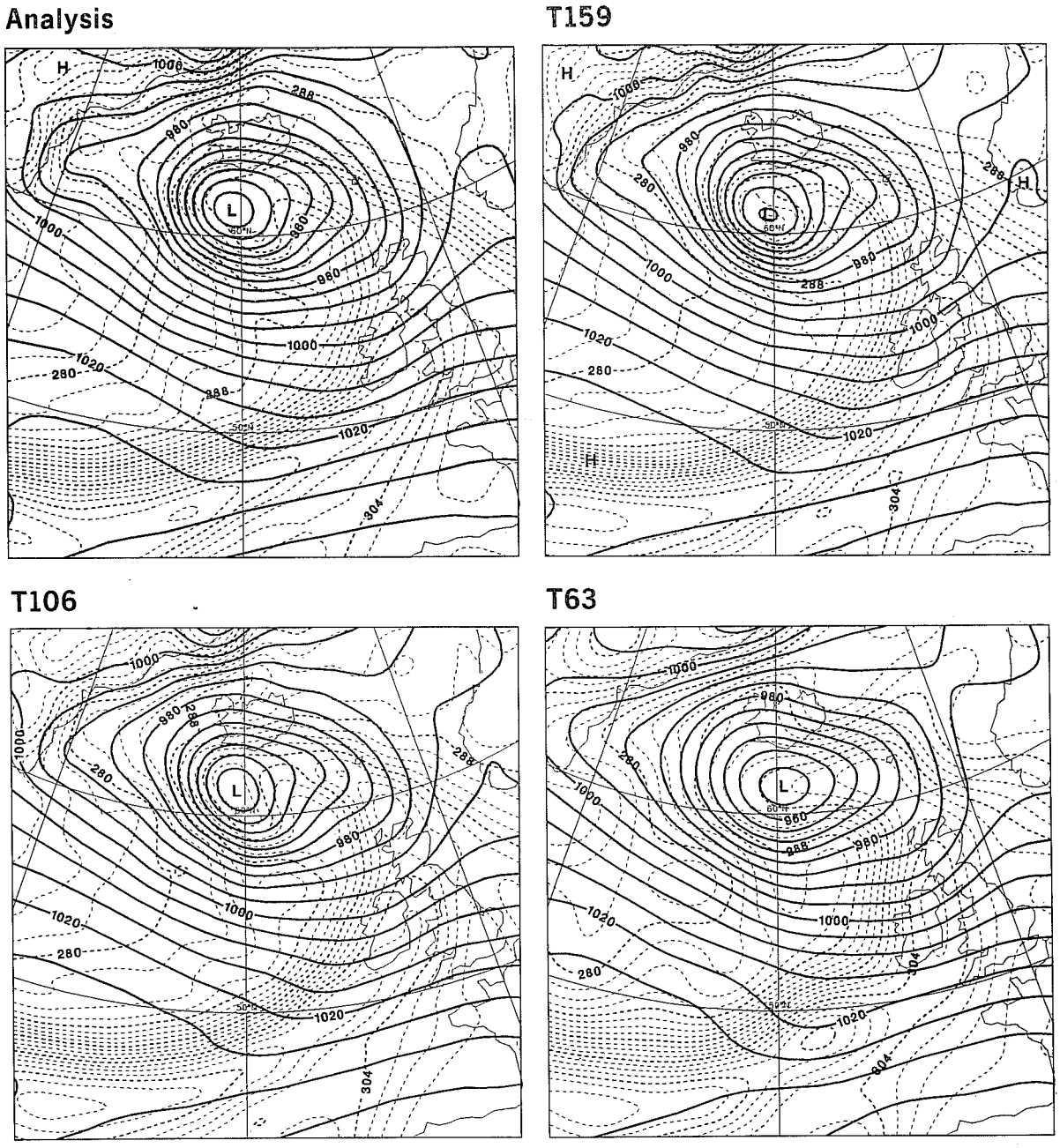

Fig. 18 The analysis of mean sea-level pressure and 850 hPa equivalent potential temperature for 13 January 1986 (upper left), and one-day T159 (upper right), T106 (lower left) and T63 (lower right) forecasts verifying on this date. Contour intervals are 5hPa and 2K respectively.

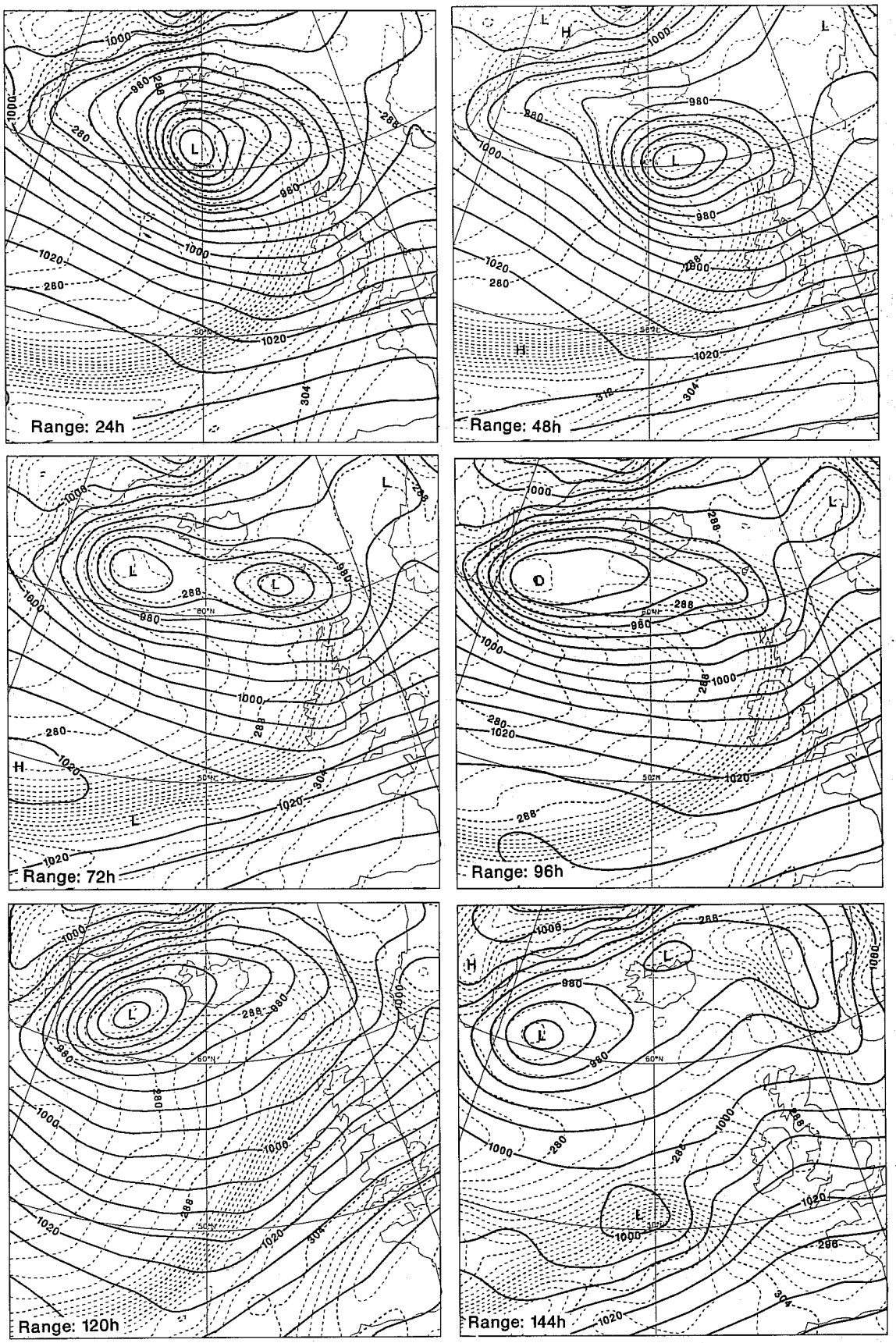

Fig. 19 Forecast maps of mean sea-level pressure (contour interval 5hPa) and 850hPa equivalent potential temperature (interval 2K) valid 12Z, 13 January 1986. Forecast ranges from 24 to 144 hours are presented.

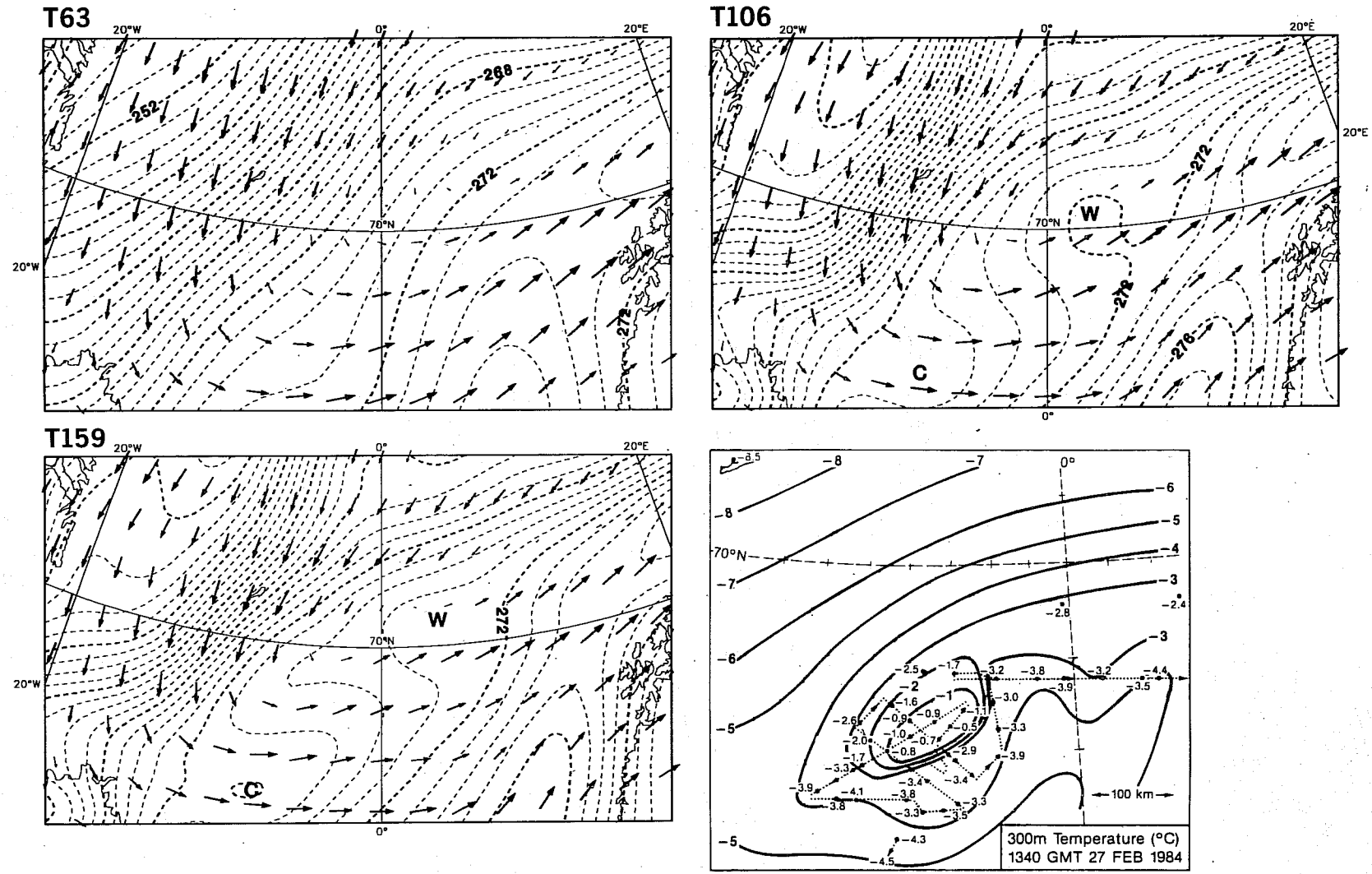

Fig. 20 Wind arrows and temperature contours (interval 1K) for model level 17 (a height of approximately 370m) for 1-day T63 (upper left), T106 (upper right) and T159 (lower left) forecasts from 12Z, 26 February 1984. An analysis by Shapiro et al (1987) of aircraft measurements taken at 300m shortly after this time is shown (for a smaller domain) in the lower right panel.

Three days before the case discussed above there was a similar rapid development over the central North Atlantic. Much the same conclusions have been found from study of the earlier case, although in this instance findings were complicated by a quite pronounced sensitivity of the detail of the development to the assimilation of the observational data in the region.

b) A polar low

The example presented here is drawn from a number of cases examined recently for sensitivity to horizontal resolution. This particular case was chosen because of the availability of detailed observations of a polar low, reported by Shapiro et al. (1987), and discussed by Reed in these Proceedings. It was recognized that none of the global resolutions that could be used would be sufficiently fine to capture the detailed structure of the low, but it was hoped that the large-scale state would be well enough defined in the initial conditions to make the case a suitable one for studying higher resolution and the performance of different convection schemes using the spectral limited-area model being developed at ECMWF. A spell of data assimilation using the latest operational system was used to produce initial conditions.

Wind and temperature forecasts using T63, T106 and T159 resolutions are shown in Fig. 20 at the third model level above the surface for 12Z, 27 February 1984, over the Norwegian Sea. Also shown is an analysis of aircraft measurements of temperature taken at a rather similar height and time. The sharpening of thermal structures with increasing resolution is evident, and more rapid spatial changes in wind speed and direction can be discerned for higher resolution. At T159 resolution a warm tongue extends southeastwards from close to the intersection of the Grenwich Meridian and the 70°N latitude, a feature clearly present in reality.

c) Hurricane movement and reintensification

As an essentially tropical phenomenon, the nature of the hurricane is not a prime topic for this seminar. However, as these systems can pose forecasting problems when they move into middle latitudes in their mature phase, two examples are considered briefly here.

Such situations are prime candidates for the study of increased horizontal resolution. A set of global forecasts has been carried out to study the

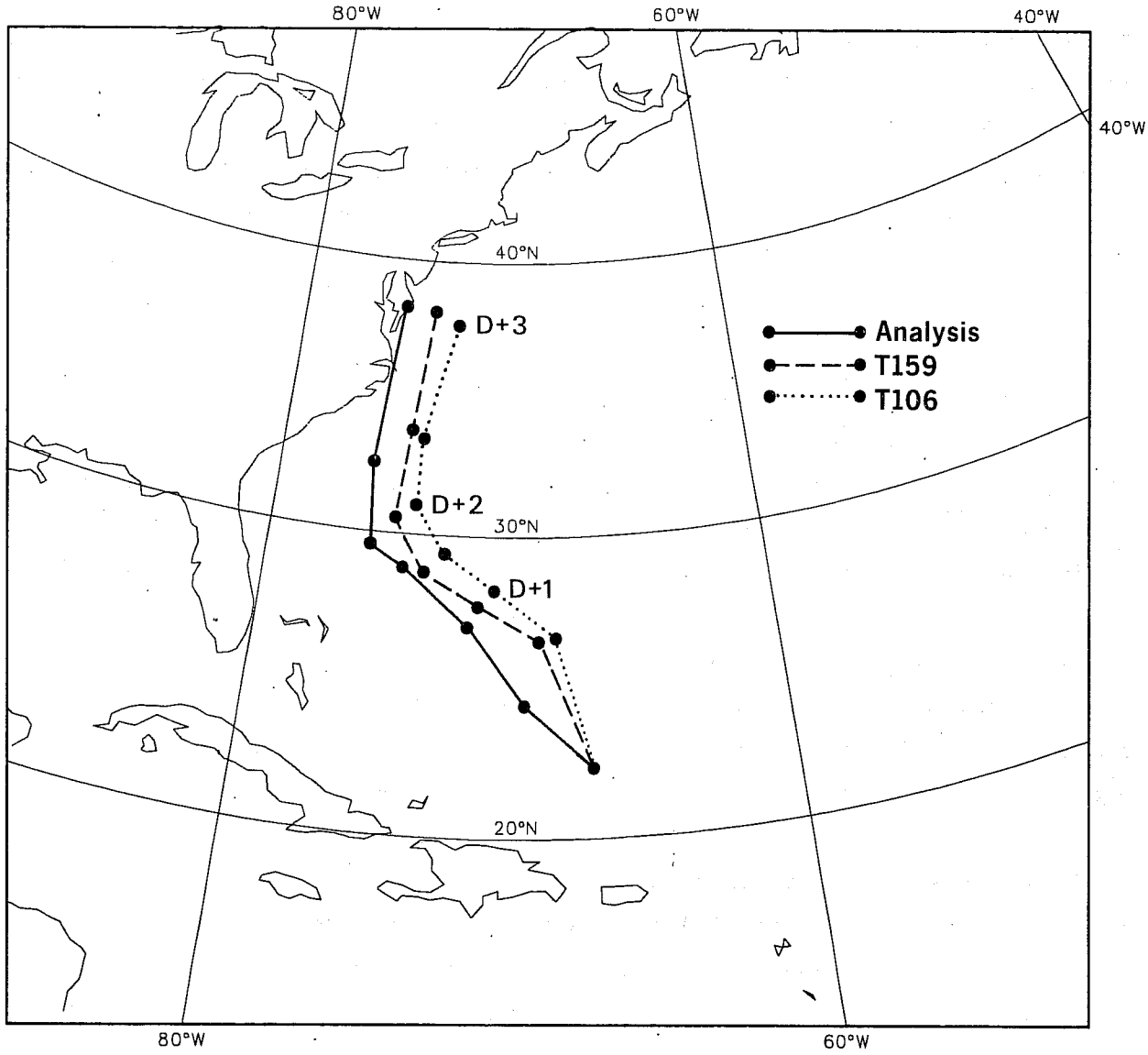

Fig. 21 Tracks of hurricane "Gloria" as analyzed operationally (solid line) for the period from 12Z, 24 September to 12Z, 27 September 1985 and as forecast from 12Z, 24 September using T106 (dotted) and T159 (dashed) resolutions.

evolution of hurricane "Gloria" from 24 to 27 September 1985 as it moved towards and then along the eastern seaboard of the USA. The analyzed track of the storm, and the tracks predicted by T106 and T159, are shown in Fig. 21. The better track of the T159 forecast, coupled with a greater (and more realistic) intensity of the system, resulted in a substantial difference in the amount of rainfall forecast over the east Coast. This can be seen in maps of the T106 and T159 predictions of precipitation for the 12-hour period leading up to 12Z, 27 September, presented in Fig. 22. This figure also includes plotted surface weather reports for 12Z on this day. Differences between T106 and T159 can also be seen in the precipitation patterns over and to the north of the Great Lakes. Comparison with the surface reports shown in Fig. 22 and those of earlier hours indicates that here also the T159 pattern is the more correct.

A particular forecasting problem for western Europe is the occasional development of intense storms in late summer and autumn arising from the interaction between an upper-air trough and a surface perturbation deriving from the remnants of a hurricane which has moved out of the tropics and into the westerly flow over the Atlantic. An example of how a complete failure to capture such an event can occur quite early in the medium range is shown in Fig. 23. The analysis maps (left panels) present the situation for 12Z, 26 August 1985, following strong development evolving from the remains of Hurricane "Charley". The forecast from four days earlier shows the British Isles under the influence of a benign surface anticyclone, an indication of development only appearing in the forecast from 27 August. Short-range guidance from the 48- and 24-hour forecasts was good.

5. TWO CASES OF BLOCKING

a) Misrepresentation of a transient wave and blocking

Attention was drawn to this case, with initial date 11 June 1986, by the failure of the operational forecast to establish high pressure centred over southern Scandinavia. A daily sequence of maps showing the analysed 500 hPa height field for the period from 11 to 16 June is presented in Fig. 24. The feature to note is the trough which crosses the Atlantic in the southern half of the domain illustrated, with an apparently shortening wavelength. This trough develops a strong northwest to southeast tilt, and the high pressure develops ahead of it. A cut-off low, originating from the preceding short-wave trough evident in the first two maps, moves slowly towards the west over the Mediterranean.

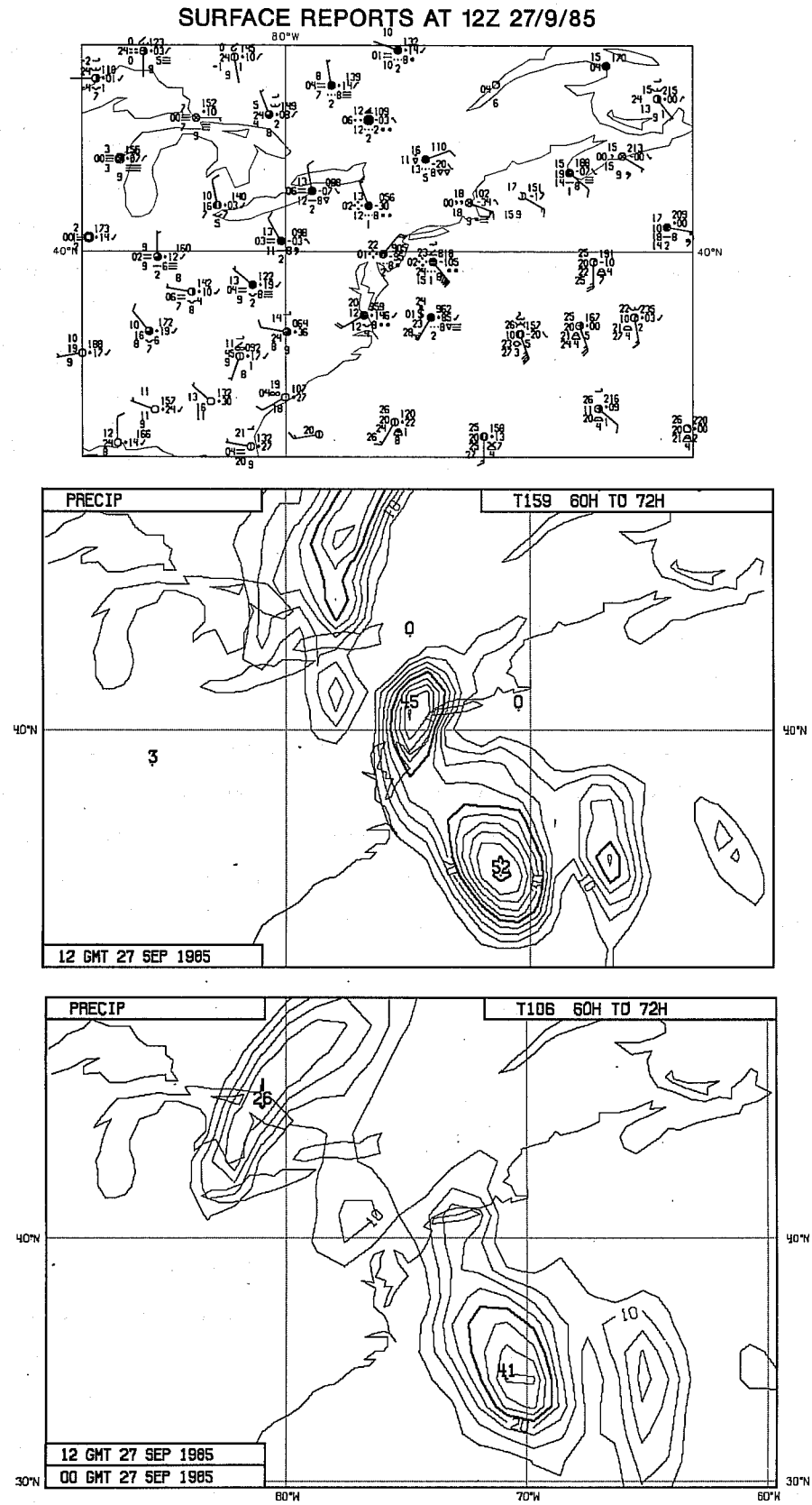

Fig. 22 Surface weather reports at 12Z, 27 September 1985, and precipitation (mm) for the period 00 to 12Z produced by T159 (middle) and T106 (lower) forecasts from 12Z, 24 September.

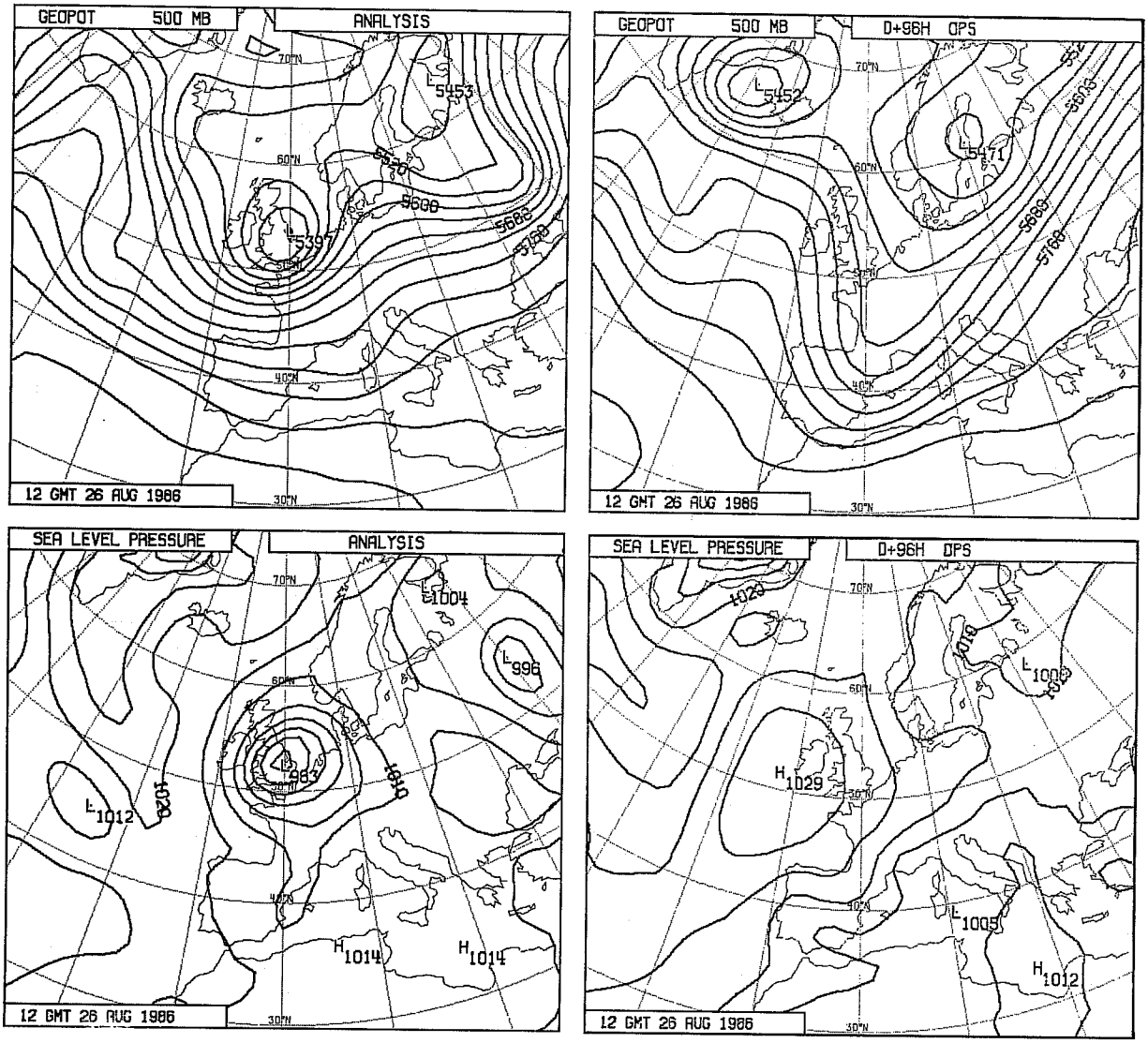

Fig. 23 500hPa height (upper, contour interval 40m) and mean sea-level pressure (lower, interval 5hPa) for 12Z, 26 August 1986. The operational analysis is shown left, and the 96-hour operational forecast valid at this time is shown right.

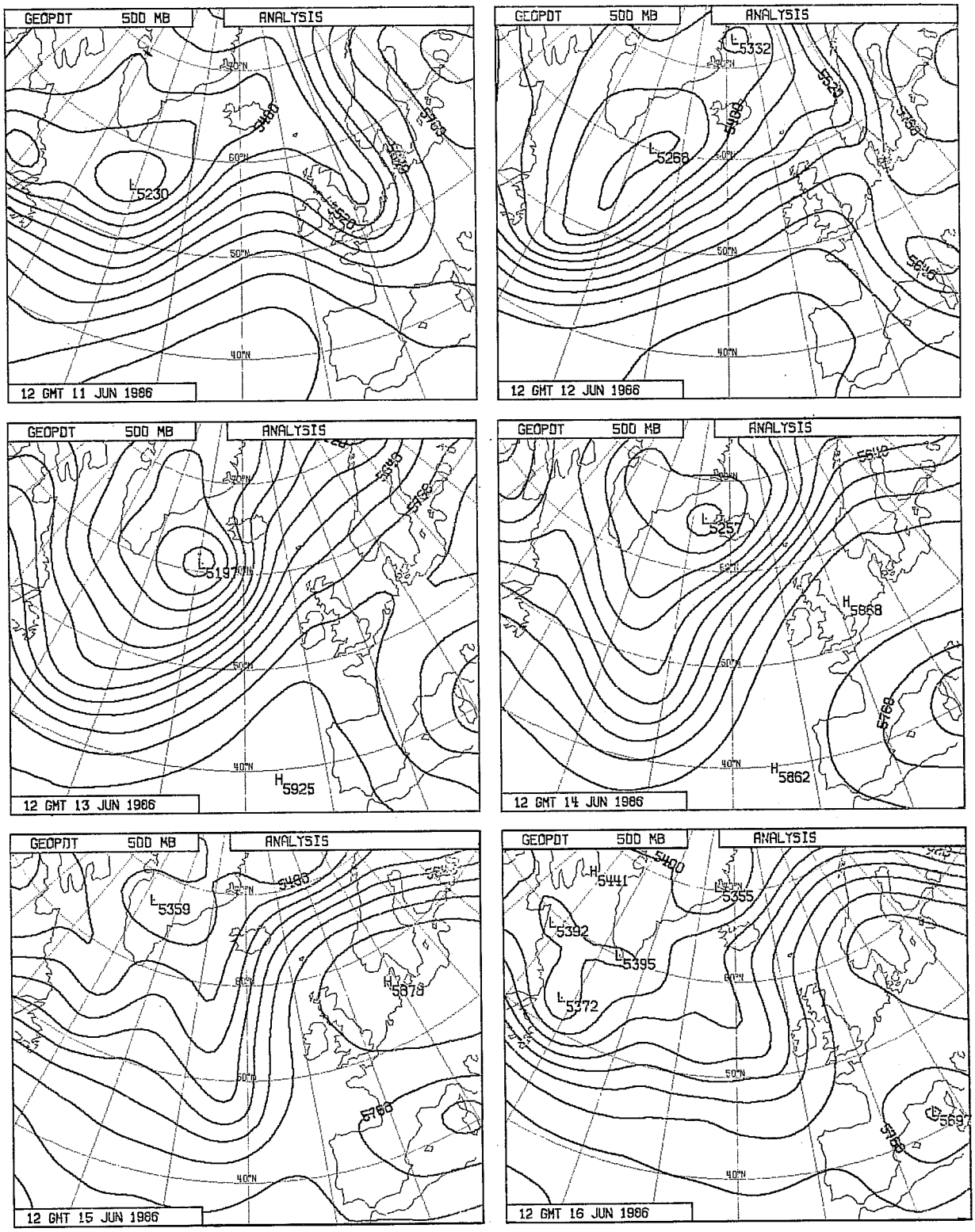

Fig. 24 500hPa height analyses (contour interval 60m) at daily intervals for the period 12Z, 11 June to 12Z 16 June 1986.

The operational forecasts for days 3, 4 and 5 (14 to 16 June) are shown in the left-hand plots of Fig. 25. By day 3 there is a significant phase-lag in the southern part of the mid-Atlantic trough, which is oriented north-south, rather than northwest-southeast. A cut-off can be seen at day 4, with high pressure west of the British Isles, which is maintained there for the duration of the forecast. Westerly flow penetrates southern Scandinavia by day 5.

The right hand panels of Fig. 25 show corresponding forecasts produced by replacing the Kuo convection scheme by the Betts-Miller scheme. The trough at day 3 is clearly positioned better with the latter scheme than in the operational forecast, and the subsequent evolution of the revised forecast follows reality quite closely. Maps of the differences between the two forecasts show that these differences develop first in the trough (initially over eastern North America) and subsequently downstream over Scandinavia.

It was also noted at the time of this poor operational forecast that the corresponding forecast produced by the UK Meteorological Office was substantially better. With the collaboration of the Meteorological Office, its operational analysis for 12Z, 11 June was converted to a form from which a forecast could be carried out with the ECMWF forecast model. This forecast was made using T63 horizontal resolution, but Fig. 26 shows how T63 and T106 forecasts from the Centre's analysis are almost identically in error when the Kuo convection scheme is used. Also shown in Fig. 26 is the T63 forecast (also using the Kuo scheme) from the Meteorological Office analysis. The improvement is striking.

It thus appears that a much better forecast can be produced in this case either by a change in parametrization or by a change in analysis. In the early stages of the forecasts, differences in convective precipitation occur in the neighbourhood of the Great Lakes between the two T106 forecasts with the different convection schemes and between the T63 forecasts from the two different analyses. Similarities can be seen between the T63 and T106 forecasts from the ECMWF analysis with the Kuo convection scheme, and to a lesser extent between the T106 forecast with the Betts-Miller convection scheme and the T63 forecast from the Meteorological Office analysis. This suggests that the difference in thermodynamic structure between the two analyses may lead to differences in initial convective heating rates which are

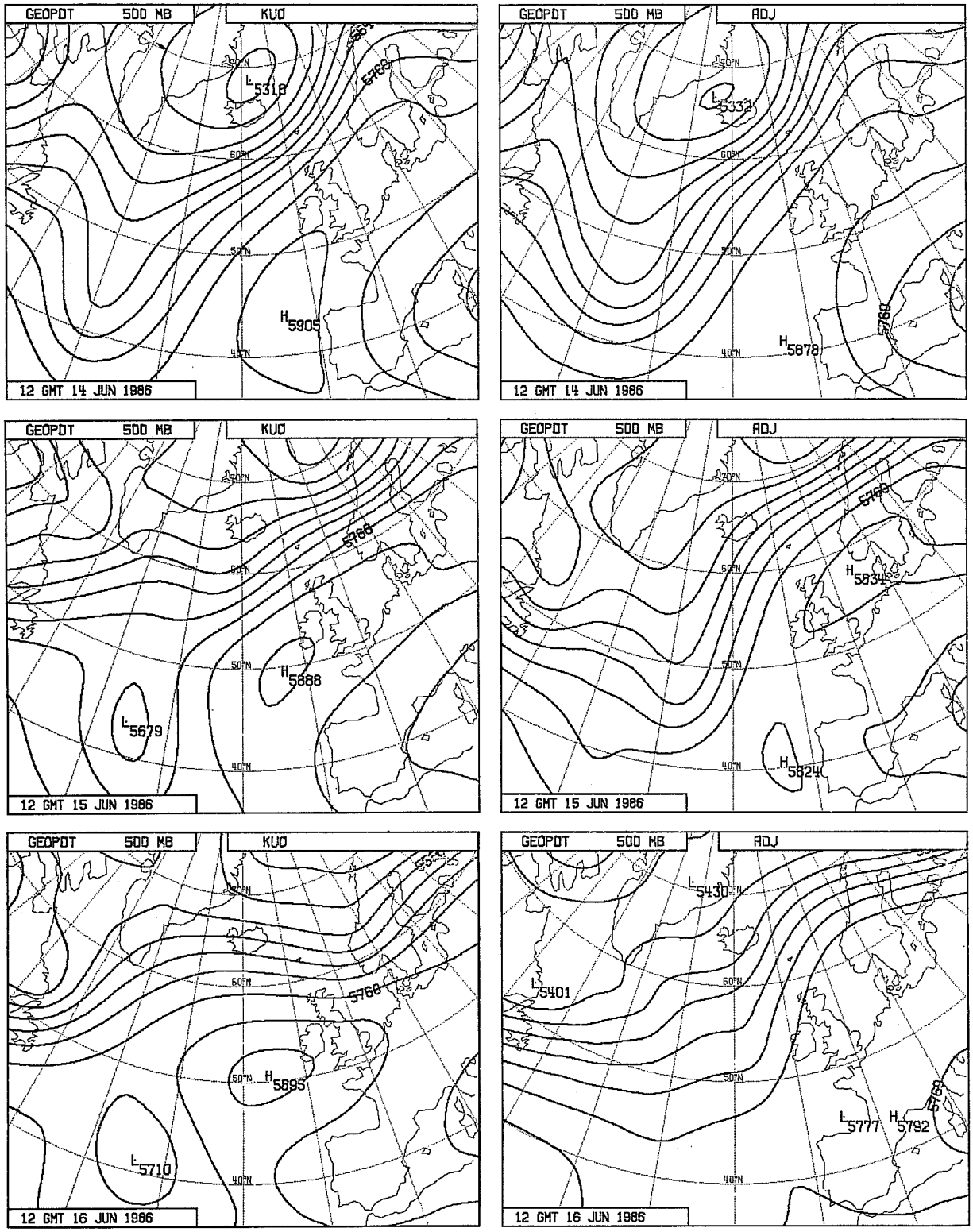

Fig. 25 500hPa height forecasts (contour interval 60m) for days 3 (upper), 4 (middle) and 5 (lower) from 12Z, 11 June, 1986, using the Kuo convection scheme (left) and the Betts-Miller scheme (right).

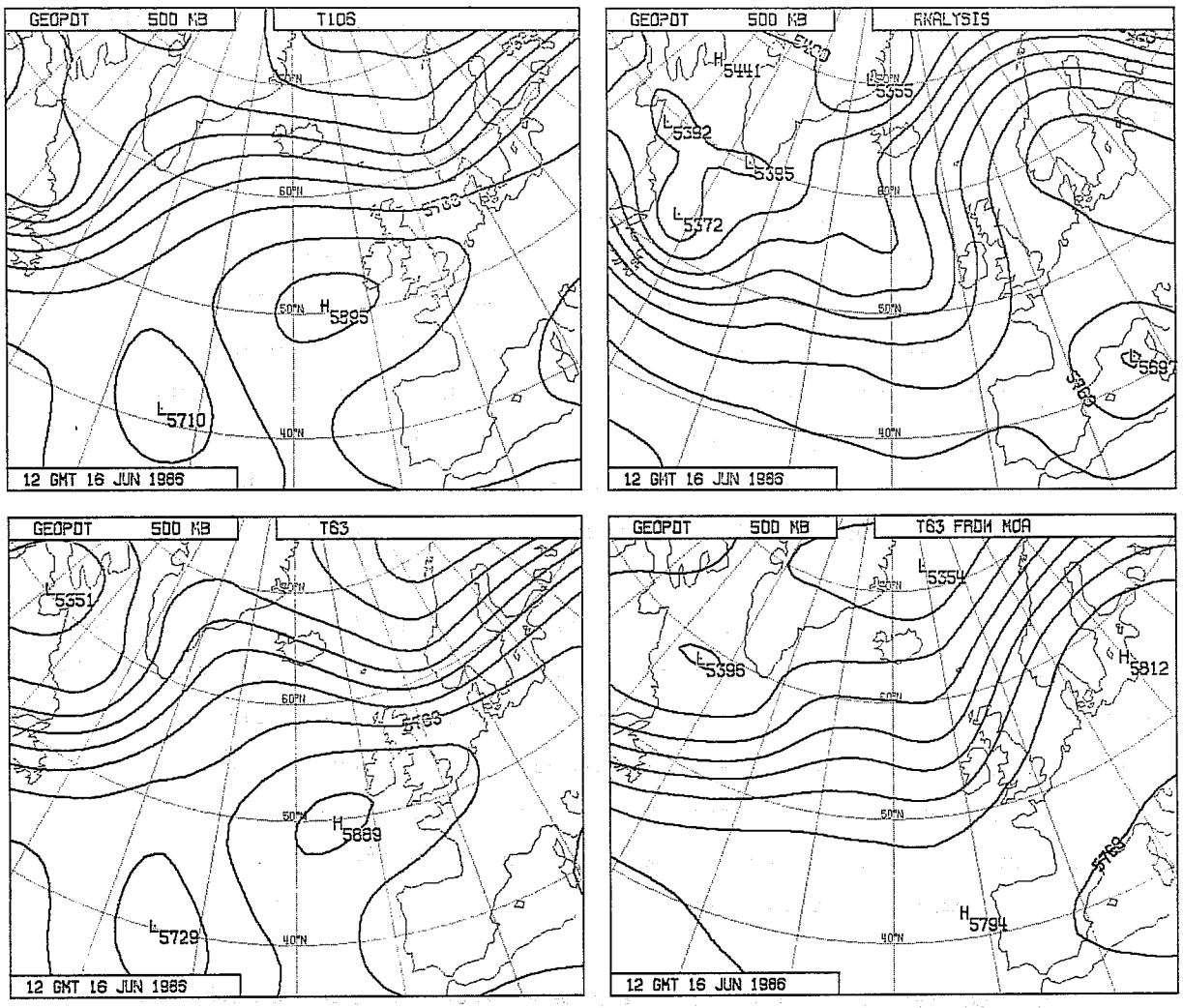

Fig. 26 500hPa height (contour interval 60m) for 12Z, 16 June 1986. The operational ECMWF analysis is shown upper right and the operational 5-day T106 forecast valid at this time is shown upper left. Lower left is the corresponding T63 forecast, and lower right a T63 forecast from the Meteorological Office analysis.

similar to differences produced by the change in parametrization. This initial heating difference may then be responsible for subsequent large forecast differences over Europe.

b) A second sensitive case

Interest was stimulated in this case by strong sensitivity found in three separate series of routine experiments, one again involving comparison of the Kuo and Betts-Miller convection schemes, one involving the comparison of T63 and T106 horizontal resolutions, and one comparing different horizontal diffusion coefficients. The sensitivity was revealed by standard objective verification of the forecasts for the extratropical Northern Hemisphere, and anomaly correlations of 500 hPa height are displayed in Fig. 27.

The upper panel shows results for the standard (operational) T106 forecast (solid line), for the corresponding T63 forecast (dashed line), and for the T106 forecast using the different convection scheme (dotted line). The latter has a substantial positive impact on forecast quality beyond day 5. Also, T63 performs significantly better than T106 in the second half of the forecast range, a result counter to the overall finding from the comparison of the resolutions (Simmons et al., 1988).

Also counter to general experience, increasing the horizontal diffusion used in the T106 model has a beneficial impact on this case. Results are shown in the lower part of Fig. 27, in which the solid line repeats the result for the operational T106 model, while the dashed line shows the result when the horizontal diffusion coefficient is doubled, in which case it takes the value used (by default) in the T63 forecast illustrated above (apart from the divergence field, for which a larger value was used for the T63 run). The dotted line in the lower panel of Fig. 27 shows the verification of a third experiment. This was motivated by diagnosis which showed that the operational T106 forecast exhibited an unusually strong "spin-up" of vertical velocity in the early stages of the forecast in the tropics. This spin-up is reduced when horizontal diffusion is increased, and a T106 experiment was thus carried out in which the higher value of diffusion was used only for the first day of the forecast, the lower value was used beyond day 2, with the diffusion coefficient decreasing linearly in time from day 1 to day 2. It is this forecast for which objective verification is represented by the dotted line in

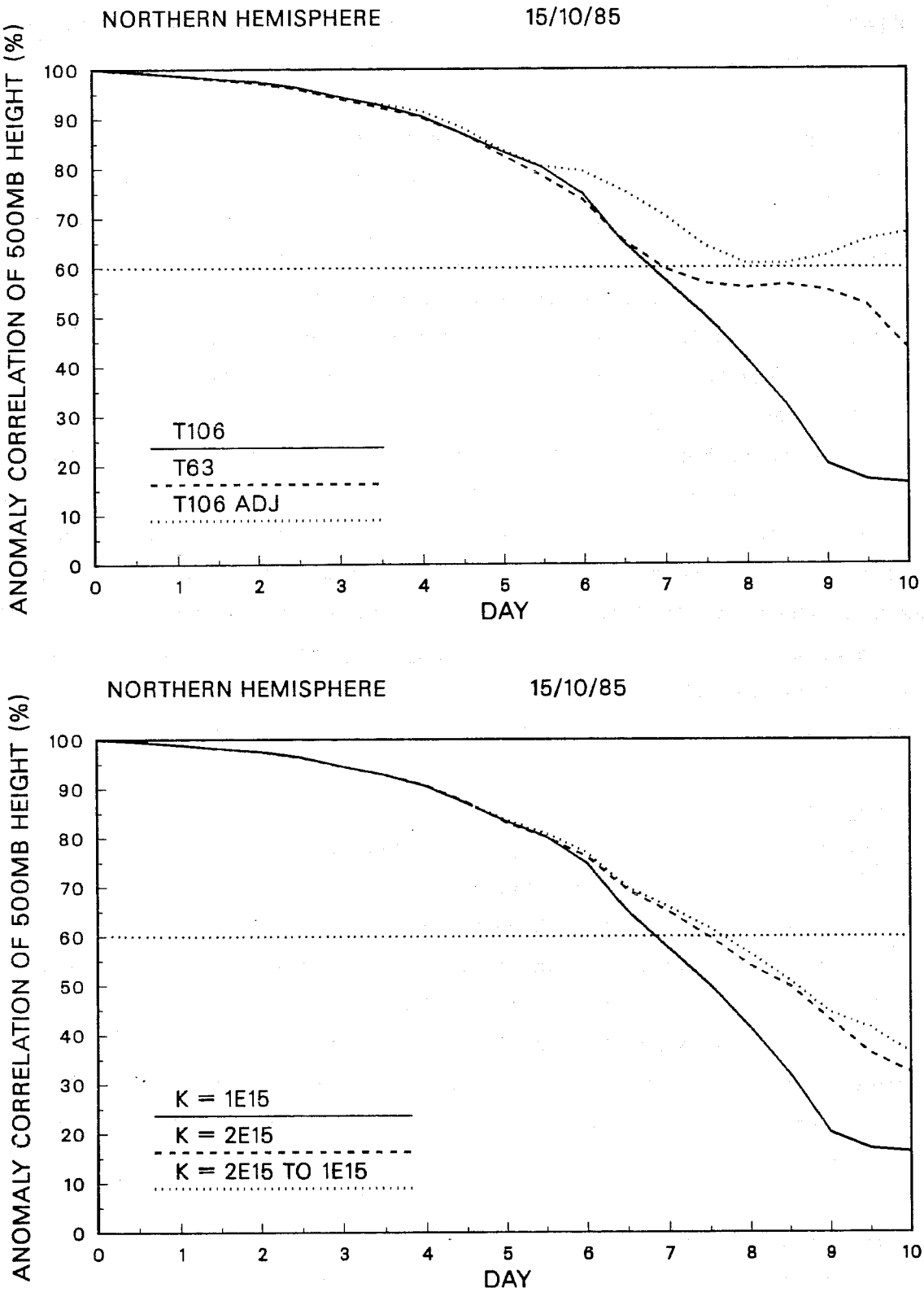

Fig. 27 Anomaly correlations of 500 hPa height for the extratropical Northern Hemisphere for a series of forecasts from 12Z, 15 October 1985. Further details are given in the text.

Fig. 27, and the results can be seen to be very close (and slightly better) than those from using the higher diffusion throughout the forecast range.

Fig. 28 presents corresponding maps of the 500 hPa height fields, averaged from days 5 to 10. Forecasts are seen to be sensitive in the Atlantic/European sector where in reality there is a sharp trough near 45°W and a blocking pattern near the Greenwich Meridian. In the standard T106 forecast, the trough is located at 60°W, pressure is high at 30°W and the circulation is cyclonic rather than anticylonic over northern Europe. The T106 forecast with the alternative convection scheme is clearly substantially better. The other maps show how the T63 forecast is intermediate in accuracy, and very similar to both of the T106 forecasts with increased horizontal diffusion. As indicated by the objective verification, the principal effect of doubling horizontal diffusion comes from its impact in the early part of the forecast range. Further investigation is needed to ascertain whether it is the differences in performance of the two convection schemes in the first day or so of the forecast that are similarly responsible for the subsequent forecast differences shown in Fig. 28. Work is also needed to identify and understand the evolution of the differences in time and space.

6. CONCLUSION

The set of cases presented in this paper should not be regarded as a representative cross-section illustrating the capability of the ECMWF forecasting system for the prediction of extratropical weather systems. The cases were chosen either on the basis of a particularly interesting weather event, or on the basis of a particular sensitivity found within a larger set of experiments, or because of a particular, striking failure of the operational forecast. Nevertheless, in so far as we have shown good forecasts as well as bad, some idea of the range of performance of the forecasting system in the prediction of cyclogenesis can be gained. Developments over recent years in data analysis and in model resolution and parametrizations have undoubtedly led to improved predictions of the formation of major storms, but failures can still occur at all time ranges, and the latter become all the more noticeable as the overall quality of forecasts rises.

Cases which are sensitive to change in some aspect of the forecast model or data assimilation provide encouraging indications of scope for future

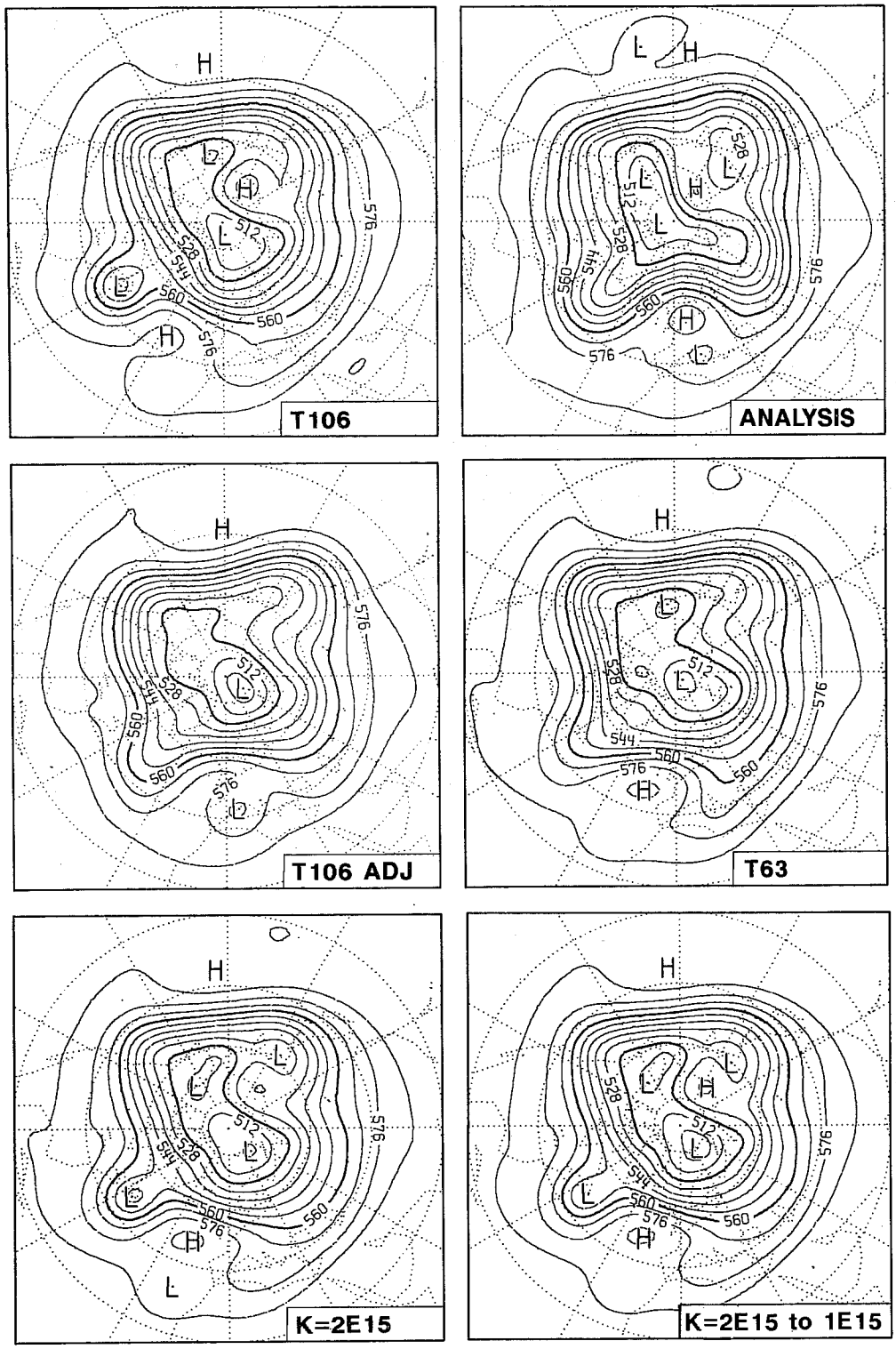

Fig. 28 Mean 500hPa height maps (contour interval 8 dam) for the period 20-25 October, 1985 for the T106 operational forecast from 15 October (upper left) and for the verifying operational analyses (upper right). The following forecasts are also shown:
Middle left: T106, with Betts-Miller convection scheme
Middle right: T63
Lower left: T106, with higher horizontal diffusion throughout range
Lower right: T106, with higher horizontal diffusion in short-range only

improvement of the operational forecasting system. Results of individual studies must, however, be viewed with caution. We have presented several examples of how similar improvements can be produced by a number of separate changes. In such circumstances, thorough understanding of the processes involved in the evolution of the event in question is necessary in order to draw firm conclusions as to the extent of any truly beneficial effect of a particular change.

Acknowledgements

The contribution of L. Dell'Osso to the study of the Presidents' Day Storm, of S. Uppala to the data assimilation for the Cleveland Storm, and of G. Sakellarides to the sensitivity of the second blocking case to horizontal diffusion, are gratefully acknowledged. We also acknowledge comments from L. Bosart on the Cleveland Storm, and collaboration with R.J. Reed in the study of the cyclogenesis over the central North Atlantic, and R. Downton in making available the analysis produced by the U.K. Meteorological Office.

References

Betts, A.K., 1986: A new convective adjustment scheme. Part I: Observational and theoretical basis. Quart.J.R.Met.Soc., 112, 677-691.

Betts, A.K. and M.J. Miller, 1986: A new convective adjustment scheme. Part II: Single column testing using GATE wave, BOMEX, ATEX and arctic air-mass data sets. Quart.J.R.Met.Soc., 112, 693-709.

Dell'Osso, L., 1984: High resolution experiments with the ECMWF model: A case study. Mon.Wea.Rev., 112, 1853-1883.

Jarraud, M., A.J. Simmons and M. Kanamitsu, 1986: Sensitivity of medium-range weather forecasts to the use of an envelope orography. ECMWF Technical Report No. 56, 83 pp.

Miller, M.J., and T.N. Palmer, 1987: Orographic gravity-wave drag: its parametrization and influence in general circulation and numerical weather prediction models. ECMWF Seminar on Observation, Theory and Modelling of Orographic Effects, Vol. 1, 283-333.

Shapiro, M.A., L.S. Fedor and T. Hampel, 1987: Research aircraft measurements of a polar low over the Norwegian Sea. Tellus, 39A, 272-306.

Simmons, A.J. and M. Jarraud, 1984: The design and performance of the new ECMWF operational model. ECMWF Seminar on Numerical Methods for Weather Prediction, Vol. 2, 113-164.

Simmons, A.J., D.M. Burridge, M. Jarraud, C. Girard and W. Wergen, 1988: The ECMWF medium-range prediction models. Development of the numerical formulations and the impact of increased resolution. To appear in Meteorology and Atmospheric Physics.

Wagner, A.J. 1978: Weather and circulation of January 1978. Mon.Wea.Rev., 106, 579-585.